J. Fluid Mech. (1984), *vol.* 145, *pp.* 151–177
Printed in Great Britain

Solute transport in heterogeneous porous formations

By GEDEON DAGAN
Faculty of Engineering, Tel-Aviv University, Tel-Aviv 69978, Israel

(Received 28 March 1983 and in revised form 20 March 1984)

Solute transport in porous formations is governed by the large-scale heterogeneity of hydraulic conductivity. The two typical lengthscales are the local one (of the order of metres) and the regional one (of the order of kilometres). The formation is modelled as a random fixed structure, to reflect the uncertainty of the space distribution of conductivity, which has a lognormal probability distribution function. A first-order perturbation approximation, valid for small log-conductivity variance, is used in order to derive closed-form expressions of the Eulerian velocity covariances for uniform average flow. The concentration expectation value is determined by using a similar approximation, and it satisfies a diffusion equation with time-dependent apparent dispersion coefficients. The longitudinal coefficients tend to constant values in both two- and three-dimensional flows only after the solute body has travelled a few tens of conductivity integral scales. This may be an exceedingly large distance in many applications for which the transient stage prevails. Comparison of theoretical results with recent field experimental data is quite satisfactory.

The variance of the space-averaged concentration over a volume V may be quite large unless the lengthscale of the initial solute body or of V is large compared with the conductivity integral scale. This condition is bound to be obeyed for transport at the local scale, in which case the concentration may be assumed to satisfy the ergodic hypothesis. This is not generally the case at the regional scale, and the solute concentration is subjected to large uncertainty. The usefulness of the prediction of the concentration expectation value is then quite limited and the dispersion coefficients become meaningless.

In the second part of the study, the influence of knowledge of the conductivity and head at a set of points upon transport is examined. The statistical moments of the velocity and concentration fields are computed for a subensemble of formations and for conditional probability distribution functions of conductivity and head, with measured values kept fixed at the set of measurement points. For conditional statistics the velocity is not stationary, and its mean and variance vary throughout the space, even if its unconditional mean and variance are constant. The main aim of the analysis is to examine the reduction of concentration coefficient of variation, i.e. of its uncertainty, by conditioning. It is shown that measurements of transmissivity on a grid of points can be effective in reducing concentration variance, provided that the distance between the points is smaller than two conductivity integral scales. Head conditioning has a lesser effect upon variance reduction.

PART 1. STATISTICALLY HOMOGENEOUS VELOCITY FIELDS

1. Introduction

We consider here the steady flow of a fluid that carries an inert and neutral solute through a porous medium. Within the usual macroscopic approach, the solute concentration (defined as mass of solute per volume of fluid) satisfies the dispersion equation with the effective molecular-diffusion coefficient supplemented by the pore-scale dispersion tensor. The latter represents the effect of convection through the porous structure, and it has been the object of thorough laboratory and theoretical investigations in the past (for a comprehensive review see e.g. Fried & Combarnous 1971). For a uniform macroscopic flow and sufficiently large Péclet number the theory shows that the dispersion coefficients are proportional to the velocity, the proportionality factor being a property of the medium known as the dispersivity. The longitudinal dispersivity is of the order of the pore scale, whereas the lateral one is smaller by one order of magnitude. In a typical laboratory test, one-dimensional flow is created in a homogeneous porous column and solute at constant concentration is introduced at the column entrance. By measuring the concentration as a function of time in the effluent and matching it with the standard solution of the diffusion equation, one can determine the longitudinal dispersion coefficient and subsequently the dispersivity.

In the present study we are interested in the problem of solute transport through large porous formations, as encountered in hydrological applications. The traditional approach assumed that in this case the concentration obeys the same dispersion equation, with appropriate dispersivity values.

Field tests, though complicated and costly, have been performed in the past in order to determine the dispersivity at the formation scale (a summary of such tests as reported in the literature is given by Lallemend-Barrés & Peaudecerf (1978) and a recent field experiment is discussed in §4 of the present paper). In a typical test, water at a predetermined concentration is injected into a flowing aquifer with the aid of a well, and the concentration is measured subsequently at a few downstream observation wells. Again, by matching the observed concentration as a function of time with the solution of the dispersion equation, values of dispersivity are found by best-fitting. A first important finding of the field experiments is that dispersivity values are generally larger than laboratory ones by a few orders of magnitude, making the latter of little value in applications. For this reason the field process has been also called 'megadispersion', in contrast with pore-scale dispersion. This discrepancy has been attributed to heterogeneity of the larger scales prevailing in natural formations, but only recently has the effect of heterogeneity been studied in a systematic, quantitative manner. A second, and disturbing, finding is that in a given formation the dispersivity varies with the distance from the solute input zone.

These results have cast doubts on the validity of the dispersion equation of transport through porous formations and have motivated a closer scrutiny of the foundations of the theory. The basic idea was to consider the effect of large-scale heterogeneity, more precisely the spatial variability of the relevant formation properties (hydraulic conductivity, porosity), and its impact upon solute transport. It is only in the last few years that formation heterogeneity has been investigated systematically, and on this basis, quantitative models of the transport process have been also developed recently.

The aim of the present study is to investigate in a systematic manner the

relationship between transport and spatial variability of the hydraulic conductivity K. In the first part K is assumed to be a stationary random function and the average flow is assumed to be uniform. The equation satisfied by the concentration expectation value is derived along the lines of Taylor's (1921) theory of diffusion by continuous movements. The procedure is illustrated for a particular autocorrelation K-function in §4 and results are subsequently compared with a recent field test. After a brief literature survey (§5), the calculation of the concentration variance and the validity of the ergodic hypothesis are discussed in §6. The main finding is that for transport at the regional scale the concentration variance may be quite large, and the ergodic hypothesis, which has been adopted in most previous studies, does not hold.

The second part of the paper examines for the first time the influence of measurements of hydraulic conductivity and pressure head at a set of points upon the statistical moments of the concentration field. A systematic procedure to assess the impact of measurements upon uncertainty is developed by using conditional probability theory. This topic departs from the traditional approach of theory of diffusion by continuous movements and might be of interest for various applications in which transport is dominated by large-scale motions.

2. Statistical characterization of the formation structure

We consider here flow through saturated porous formations of aquifers that have two typical dimensions: a vertical thickness of the order of tens to hundreds of metres and a horizontal extent of the order of kilometres. We therefore ignore heterogeneity at the pore scale and regard the fluid and the solute as continua. The hydraulic conductivity and porosity determined with the aid of cores or samples are regarded as point values. Whenever such measurements are carried out at different locations of a natural formation, it is found that the properties vary in an irregular manner in space, i.e. as a rule formations are heterogeneous.

There are two different and distinct scales of heterogeneity. The local scale refers to changes throughout the depth of the aquifer and over horizontal distances of the same order. A sampling of the properties (hydraulic conductivity, porosity) at this scale can be carried out by extracting cores at different points and measuring their properties in the laboratory. Then it is found that the spatial correlation scale is of the order of metres or tens of metres. The structure is essentially three-dimensional, but horizontal layering often creates a pronounced anisotropy, with the scale of horizontal correlations much larger than the vertical one. In §4 we shall describe a field test in which this was apparently the case.

In contrast, in most hydrological applications we are interested in processes at the regional scale, which is of the order of the horizontal extent of the formation. This scale is much larger than the depth, and the formation properties, as well as flow variables, are averaged over the depth and regarded as functions only of two dimensions in the plane, in a similar way to the shallow-water approximation. Then, hydraulic conductivity is replaced by transmissivity, and the latter is determined as a rule by pumping tests. Obviously, the local heterogeneity is wiped out in such a process, and new correlation scales characterizing heterogeneity, of the order of hundreds to thousands of metres, are found out.

To account for variability and uncertainty, the formation properties are regarded as spatial random functions. A survey of field data found in the literature for properties at the local scale has been presented by Freeze (1975). It has been found that hydraulic conductivity K has a lognormal probability density function. With

$Y = \ln K$, the variance σ_Y^2 has been found to reach values as large as 13 in some formations, although most figures are more moderate. Fewer data are available with regard to the porosity n, and Freeze (1975) suggests that it is linearly correlated to Y. The correlation coefficient is such that $\sigma_n^2 = 1.12 \times 10^{-4} \sigma_Y^2$, i.e. the porosity is much less variable than the hydraulic conductivity.

Data about the regional-scale heterogeneity have been summarized by Delhomme (1979) for a few aquifers in France. Again, the lognormal distribution is found to represent realistically the p.d.f. of the transmissivity with variance values between 0.7 and 5. Delhomme also mentions correlation scales in the horizontal plane in the range 1–20 km. Clifton & Neuman (1982) have analysed data obtained from 148 wells in the Avra Valley, the thickness of the aquifer being around 200 m and its horizontal extent of the order of tens of kilometres. The variance of the log-transmissivity was found to be around 0.5, whereas the correlation scale was of the order of 8 km.

On the basis of this picture, we shall regard here a porous formation, at both local and regional scales, as a realization of an ensemble of formations of random structures. The randomness reflects the uncertainty of the values of the hydraulic conductivity or transmissivity in space. In line with the aforementioned field findings and various recent works on stochastic modelling of groundwater flow (for a brief review see e.g. Dagan 1982*a*), we shall assume that the logarithm of the hydraulic conductivity, at the local scale, or of the transmissivity at the regional scale, has a normal unconditional probability density function with mean m_Y and a constant variance σ_Y^2. The values of $Y' = Y - m_Y$ at N points $\boldsymbol{x}_1, \boldsymbol{x}_2, \ldots, \boldsymbol{x}_N$ have a multivariate normal distribution with a covariance matrix which can be derived from the unconditional autocovariance function $C_Y(\boldsymbol{r})$. The latter is supposed to depend on the distance or the lag vector $\boldsymbol{r}$ between the two points. To simplify matters we shall also adopt in a few numerical applications the exponential autocorrelation, suggested in previous works, namely $C_Y = \sigma_Y^2 \exp(-|\boldsymbol{r}|/I_Y)$, where I_Y is the linear integral scale of Y'. Thus, in this simplest representation $Y'(\boldsymbol{x})$ is a two- or three-dimensional stationary and isotropic random function, determined entirely by the two numbers σ_Y^2 and I_Y. The ensemble mean m_Y is generally a smooth and slowly varying function of $\boldsymbol{x}$, which for simplicity can also be taken constant.

We disregard here the uncertainty associated with measurement errors or other sources resulting in spatially uncorrelated fluctuations of Y, since they do not affect the transport process. Futhermore, we shall neglect the spatial variability of the porosity, which has a negligible effect upon the spread of the solute as compared with that of Y.

3. Mathematical statement of the problem and first-order solution

We consider here a porous formation within a domain Ω bounded by a surface Σ. Let $\boldsymbol{x}$ be the Cartesian coordinate vector of a point, with x, y or x, y, z its components in the two- or three-dimensional space respectively (we shall also use occasionally the suffix notation x_1, x_2 and x_1, x_2, x_3). We consider here steady flows, such that the flow equations, in absence of recharge, are

$$\boldsymbol{q} = -K \nabla \Phi, \quad \nabla \cdot \boldsymbol{q} = 0, \tag{3.1}$$

where $\Phi = p/\gamma + z$ is the head, p is the pressure, γ is the fluid specific weight, z is the elevation, and $\boldsymbol{q}$ is the specific discharge. As before, K is the hydraulic conductivity $k\gamma/\mu$, where k is the permeability and μ is the coefficient of dynamic viscosity of the fluid. In the case of two-dimensional flow at the regional scale, Φ and $\boldsymbol{q}$ are averaged over depth, whereas K is the ratio between transmissivity and depth.

Assuming for the sake of simplicity a uniform head gradient $-\boldsymbol{J}$ on the boundary Σ and defining the head fluctuation ϕ by $\phi = \Phi + \boldsymbol{J}\cdot\boldsymbol{x}$, elimination of $\boldsymbol{q}$ from (3.1) yields

$$\left.\begin{aligned} \nabla^2\phi + \nabla Y\cdot\nabla\phi &= \boldsymbol{J}\cdot\nabla Y \quad (\boldsymbol{x}\in\Omega), \\ \phi &= 0 \quad (\boldsymbol{x}\in\Sigma), \end{aligned}\right\} \tag{3.2}$$

where $Y = \ln K$.

The filtration velocity $\boldsymbol{U}$ is defined by $\boldsymbol{U} = \boldsymbol{q}/n$, where the effective porosity n is assumed to be constant. The solution of the transport problem requires the computation of the velocity covariances

$$u_{jk}(\boldsymbol{x},\boldsymbol{y}) = \langle u_j(\boldsymbol{x})\, u_k(\boldsymbol{y})\rangle, \quad \boldsymbol{u} = \boldsymbol{U} - \langle \boldsymbol{U}\rangle, \tag{3.3}$$

which have to be evaluated in terms of the random function $Y = \ln K$. The solution of the stochastic differential equation (3.2), giving the moments of ϕ as functions of those of Y, is one of the central problems of the theory of heterogeneous media (see e.g. Beran 1968). In particular, the covariances

$$C_{Y\phi}(\boldsymbol{x},\boldsymbol{y};\sigma_Y^2) = \langle Y'(\boldsymbol{x})\,\phi(\boldsymbol{y})\rangle, \quad C_\phi(\boldsymbol{x},\boldsymbol{y};\sigma_Y^2) = \langle \phi(\boldsymbol{x})\,\phi(\boldsymbol{y})\rangle \tag{3.4}$$

depend in a nonlinear fashion upon the log-conductivity variance. We shall limit the present study to a linearized, first-order approximation of ϕ, such that

$$C_{Y\phi} = \sigma_Y^2\, c_{Y\phi}(\boldsymbol{x},\boldsymbol{y}), \quad C_\phi = \sigma_Y^2\, c_\phi(\boldsymbol{x},\boldsymbol{y}). \tag{3.5}$$

This approximation simplifies considerably the computations and permits one to obtain closed-form solutions and to grasp the main features of the transport phenomenon. Furthermore, the results may be applied to porous formations for which $\sigma_Y^2 < 1$, and they may also constitute the starting point of involved, numerical solutions. The functions $c_{Y\phi}$ and c_ϕ in (3.5) can be obtained explicitly from the linearized version of (3.2):

$$\left.\begin{aligned} \nabla^2\phi &= \boldsymbol{J}\cdot\nabla Y \quad (\boldsymbol{x}\in\Omega); \\ \phi &= 0 \quad (\boldsymbol{x}\in\Sigma). \end{aligned}\right\} \tag{3.6}$$

To simplify notation the average flow is assumed to be in the x-direction and variables are made dimensionless with respect to the integral scale l_Y as a lengthscale, Jl_Y as head scale and $\langle U\rangle = J\exp(m_Y)/n$ as velocity scale. The solution of (3.6) is then given by

$$\phi(\boldsymbol{x}) = -\int_\Omega \frac{\partial Y'(\boldsymbol{x}')}{\partial x'} G(\boldsymbol{x},\boldsymbol{x}')\,\mathrm{d}\boldsymbol{x}' = \int_\Omega Y'(\boldsymbol{x}')\frac{\partial G(\boldsymbol{x},\boldsymbol{x}')}{\partial x'}\,\mathrm{d}\boldsymbol{x}', \tag{3.7}$$

where $G(\boldsymbol{x},\boldsymbol{x}')$ is the Green function for Laplace's equation. The covariances (3.5) are therefore given by

$$\left.\begin{aligned} c_{Y\phi}(\boldsymbol{x},\boldsymbol{y}) &= \int_\Omega c_Y(\boldsymbol{x},\boldsymbol{x}')\frac{\partial G(\boldsymbol{y},\boldsymbol{x}')}{\partial x'}\,\mathrm{d}\boldsymbol{x}', \\ c_\phi(\boldsymbol{x},\boldsymbol{y}) &= \int\int_\Omega c_Y(\boldsymbol{x}',\boldsymbol{x}'')\frac{\partial G(\boldsymbol{x},\boldsymbol{x}')}{\partial x'}\frac{\partial G(\boldsymbol{y},\boldsymbol{x}'')}{\partial x''}\,\mathrm{d}\boldsymbol{x}'\,\mathrm{d}\boldsymbol{x}''. \end{aligned}\right\} \tag{3.8}$$

To simplify matters further we let the domain Ω expand to infinity, with G given by

$$G(\boldsymbol{x},\boldsymbol{x}') = -\frac{1}{2\pi}\ln(|\boldsymbol{x}-\boldsymbol{x}'|), \quad G(\boldsymbol{x},\boldsymbol{x}') = \frac{1}{4\pi}\frac{1}{|\boldsymbol{x}-\boldsymbol{x}'|} \tag{3.9}$$

for the two- and three-dimensional spaces respectively. It is immediately seen that, for stationary Y, $c_{Y\phi}$ is a function of $\boldsymbol{x}-\boldsymbol{y}$ and is generally finite. In contrast, c_ϕ

becomes unbounded in an infinite two-dimensional domain. Since only the head derivatives or increments are needed here, a convenient way to circumvent this difficulty is the one adopted in geostatistics (see e.g. Journel & Huijbregts 1978) to take advantage of the fact that ϕ has stationary increments. The variogram Γ_ϕ (known also as the semivariogram) is defined by

$$\Gamma_\phi(\boldsymbol{x},\boldsymbol{y};\sigma_Y^2) = \sigma_Y^2\gamma_\phi(\boldsymbol{x},\boldsymbol{y}) = \tfrac{1}{2}\langle[\phi(\boldsymbol{x})-\phi(\boldsymbol{y})]^2\rangle = \tfrac{1}{2}[\sigma_\phi^2(\boldsymbol{x})+\sigma_\phi^2(\boldsymbol{y})-2C_\phi(\boldsymbol{x},\boldsymbol{y})], \quad (3.10)$$

and it tends to the following finite limit for an infinite domain:

$$\gamma_\phi(\boldsymbol{x}-\boldsymbol{y}) = \int\int c_Y(\boldsymbol{x}'')\left[\frac{\partial G(\boldsymbol{x}')}{\partial x'}\frac{\partial G(\boldsymbol{x}'-\boldsymbol{x}'')}{\partial x''} - \frac{\partial G(\boldsymbol{x}')}{\partial x'}\frac{\partial G(\boldsymbol{x}'-\boldsymbol{x}''+\boldsymbol{x}-\boldsymbol{y})}{\partial x''}\right]\mathrm{d}\boldsymbol{x}'\,\mathrm{d}\boldsymbol{x}''. \quad (3.11)$$

It follows from the linearity of (3.7) that the increments of ϕ are normal since Y is normal. Therefore the joint probability density function of Y and the increment of ϕ are completely defined with the aid of c_Y and the associated $c_{Y\phi}$ and γ_ϕ.

By the same first-order approximation the velocity fluctuation is found from (3.1) as

$$\boldsymbol{u}(\boldsymbol{x}) = Y'(\boldsymbol{x})\,\boldsymbol{i} - \nabla\phi(\boldsymbol{x}), \quad \langle \boldsymbol{U}\rangle = \boldsymbol{i}, \quad (3.12)$$

where $\boldsymbol{i}$ is a unit vector in the x-direction. Finally, by using (3.8), (3.11) and (3.12), the velocity covariances have the following first-order expressions:

$$u_{jk}(\boldsymbol{x},\boldsymbol{y}) = \sigma_Y^2\left[\delta_{1j}\delta_{1k}\,c_Y(\boldsymbol{x},\boldsymbol{y}) - \delta_{1j}\frac{\partial c_{Y\phi}(\boldsymbol{x},\boldsymbol{y})}{\partial y_k} - \delta_{1k}\frac{\partial c_{Y\phi}(\boldsymbol{y},\boldsymbol{x})}{\partial x_j} - \frac{\partial^2\gamma_\phi(\boldsymbol{x},\boldsymbol{y})}{\partial x_j\partial y_k}\right], \quad (3.13)$$

where δ_{jk} is the Kronecker delta and $j, k = 1, \ldots, m$ with $m = 2$ (2-dimensional) and $m = 3$ (3-dimensional).

Again, $\boldsymbol{u}$ is Gaussian and its p.d.f. is defined entirely by u_{jk}, which in turn is given explicitly as a function of c_Y. Equation (3.13) is the starting point for both parts of the present study.

After these preparatory steps the problem we are going to address here is as follows. Solute at initial concentration $c_0(\boldsymbol{x}, t_0)$ is introduced in a porous formation within a volume V_0; what is the subsequent concentration distribution $C(\boldsymbol{x},t)$ as result of convection and dispersion?

Following the standard procedure of the theory of diffusion by continuous movements, we consider first an infinitesimal solute particle of mass $\mathrm{d}M = C_0\,\mathrm{d}\boldsymbol{x}_0$. The associated concentration field is given by

$$\mathrm{d}C(\boldsymbol{x},t;\boldsymbol{x}_0,t_0) = \mathrm{d}M\,\delta[\boldsymbol{x}-\boldsymbol{X}_\mathrm{t}(t;\boldsymbol{x}_0,t_0)] \quad (3.14)$$

where δ is the Dirac distribution. The vector $\boldsymbol{X}_\mathrm{t}$ represents the displacement of the particle which started its motion at $\boldsymbol{x} = \boldsymbol{x}_0$, $t = t_0$. $\boldsymbol{X}_\mathrm{t}$ is decomposed as

$$\boldsymbol{X}_\mathrm{t}(t;\boldsymbol{x}_0,t_0) = \boldsymbol{X}(t;\boldsymbol{x}_0,t_0) + \boldsymbol{X}_\mathrm{d}(t;t_0). \quad (3.15)$$

In (3.15) $\boldsymbol{X}_\mathrm{d}$ represents the displacement associated with a 'Brownian-motion' type of diffusion process. In the present context $\boldsymbol{X}_\mathrm{d}$ is associated with the pore-scale dispersion in the case of transport at the local scale. For transport at the regional scale, $\boldsymbol{X}_\mathrm{d}$ incorporates the effect of the local-scale heterogeneity.

In contrast, $\boldsymbol{X}$ stems from convective transport by the fluid. For the steady flow of uniform average velocity defined before, $\boldsymbol{X}$ is related to the velocity field as follows:

$$\boldsymbol{X}(t;\boldsymbol{x}_0,t_0) = \boldsymbol{x}_0 + (t-t_0)\,\boldsymbol{i} + \int_0^t \boldsymbol{u}(\boldsymbol{X}_\mathrm{t})\,\mathrm{d}t'. \quad (3.16)$$

It should be remembered that $\boldsymbol{X}$ is made dimensionless by division by l_Y, the hydraulic conductivity integral scale. $\boldsymbol{X}$ is a random function and its average is given by

$$\langle \boldsymbol{X} \rangle = \boldsymbol{x}_0 + (t - t_0)\,\boldsymbol{i}, \tag{3.17}$$

i.e. the particle mean path is a straight line along the x-axis. The fluctuation $\boldsymbol{X}'(t; \boldsymbol{x}_0, t_0)$ is given by the integral in (3.16), leading to a nonlinear integral equation for $\boldsymbol{X}'$. A large body of literature has been devoted to deriving approximate relationships between the displacements and the Eulerian velocity covariances. We adopt here the simplest approach, which is consistent with the first-order approximation of the velocity field, namely we replace $\boldsymbol{X}_t$ in the integral of (3.17) by its average. Thus we obtain the fundamental relationship

$$\boldsymbol{X}'(t; \boldsymbol{x}_0, t_0) = \int_0^t \boldsymbol{u}(x_0 + t' - t_0, y_0, z_0)\,\mathrm{d}t', \tag{3.18}$$

which gives $\boldsymbol{X}'$ explicitly in terms of $\boldsymbol{u}$. Retaining additional terms in $\boldsymbol{X}_t$ in $\boldsymbol{u}$ would lead to expressions of higher order in σ_Y^2 or in the product between σ_Y^2 and the dispersion coefficient associated with the 'Brownian-motion' term. Conditions under which (3.18) might become a non-uniform approximation for large t will be discussed in §5. The convergence of an iterative procedure in which (3.18) is the first term has been discussed by Phythian (1975), with encouraging results for the case in which the velocity spectrum is sufficiently smooth.

Since $\boldsymbol{u}$ is a normal random function, the same is true for $\boldsymbol{X}'$. The p.d.f. of $\boldsymbol{X}$ can be written down as usual as

$$f(\boldsymbol{X}; t, t_0, \boldsymbol{x}_0) = \frac{1}{(2\pi)^m |X_{jk}|} \exp\left[-\frac{1}{2} \sum_{j=1}^{m} \sum_{k=1}^{m} (X_j - \langle X_j \rangle)(X_k - \langle X_k \rangle) X_{jk}^{-1} \right]. \tag{3.19}$$

Here and in the sequal $m = 2, 3$ stands for the number of dimensions of the space of the flow domain, X_{jk} is the displacement covariance tensor, $|X_{jk}|$ is its determinant and X_{jk}^{-1} is its inverse. It is easy to express X_{jk} with the aid of the velocity covariance by using (3.18) as follows:

$$\begin{aligned} X_{jk}(t; \boldsymbol{x}_0, t_0) &= \langle X_j'(t; \boldsymbol{x}_0, t_0)\, X_k'(t; \boldsymbol{x}_0, t_0) \rangle \\ &= \int_0^t \int_0^t u_{jk}(x_0 + t' - t_0, y_0, z_0, x_0 + t'' - t_0, y_0, z_0)\,\mathrm{d}t'\,\mathrm{d}t''. \end{aligned} \tag{3.20}$$

The 'Brownian-motion' component $\boldsymbol{X}_d$ in (3.15) has a zero mean and a normal p.d.f. with the covariance tensor given by

$$X_{djk}(t - t_0) = 2(t - t_0)\, D_{djk}. \tag{3.21}$$

D_{djk} is the dimensionless pore-scale or local dispersion tensor and has the nature of a Péclet number. If the dispersion coefficients are written as the dispersivities times the average velocity, D_{djk} becomes equal to the ratio between dispersivity and the integral scale l_Y, it being assumed that this ratio is much smaller than unity. Furthermore, $\boldsymbol{X}_d$ is uncorrelated with $\boldsymbol{u}$, so that we can write for the covariance of $\boldsymbol{X}_t$

$$X_{tjk} = X_{jk} + 2(t - t_0)\, D_{djk}. \tag{3.22}$$

Obviously, $\boldsymbol{X}_t$ is also normal, of mean (3.17) and covariance (3.22). We turn now to the calculation of the expectation value of the concentration $\mathrm{d}C$ (3.14). This is done

by multiplying $\mathrm{d}C$ by the p.d.f. of $\boldsymbol{X}_t$ and integrating over $\boldsymbol{X}_t$. It is immediately seen from (3.14) that we arrive at the classical result that

$$\left\langle \frac{\mathrm{d}C}{\mathrm{d}M} \right\rangle = f(\boldsymbol{x}; t, \boldsymbol{x}_0, t_0), \tag{3.23}$$

where f is the Gaussian function (3.19) in which X_{jk} is replaced by X_{tjk}.

This result can be extended immediately to a solute body introduced at $t_0 = 0$ in a finite volume V_0:

$$\langle C(\boldsymbol{x}, t) \rangle = \int_{v_0} C_0 f(\boldsymbol{x}, t; \boldsymbol{x}_0)\, \mathrm{d}\boldsymbol{x}_0, \tag{3.24}$$

and similarly, by integrating over t_0, for a plume.

Another classical result, which can be arrived at by differentiation of f (3.19), is that $\langle C(\boldsymbol{x}, t) \rangle$ satisfies the dispersion-type equation

$$\frac{\partial \langle C \rangle}{\partial t} + \frac{\partial \langle C \rangle}{\partial x} = \sum_{j=1}^{m} \sum_{k=1}^{m} D_{tjk}(t) \frac{\partial^2 \langle C \rangle}{\partial x_j \, \partial x_k}, \tag{3.25}$$

with the coefficients D_{tjk} given by

$$D_{tjk} = \frac{1}{2} \frac{\mathrm{d}X_{tjk}}{\mathrm{d}t} = \frac{1}{2} \frac{\mathrm{d}X_{jk}}{\mathrm{d}t} + D_{djk}. \tag{3.26}$$

The general results presented so far, which are based on well-established concepts, are the starting point of our analysis of transport in porous formations in the sequel.

4. An illustrative example and comparison with a field test

To illustrate the approach we adopt the particular form of log-conductivity covariance mentioned in §2 and employed in a previous work (Dagan 1982*a*), namely

$$C_Y = \sigma_Y^2 c_Y, \quad c_Y(\boldsymbol{r}) = \exp(-|\boldsymbol{r}|). \tag{4.1}$$

By substituting c_Y from (4.1) and G from (3.9) into (3.8) and (3.11) for two-dimensional flow, the following closed-form expressions are obtained after a few quadratures:

$$c_{Y\phi}(\boldsymbol{x}, \boldsymbol{y}) = c_{Y\phi}(\boldsymbol{r}) = \frac{r_x}{r^2}[(1+r)\,\mathrm{e}^{-r} - 1], \tag{4.2}$$

$$\gamma_\phi(\boldsymbol{x}, \boldsymbol{y}) = \gamma_\phi((\boldsymbol{r}) = \frac{1}{2}\left\{\frac{r_x^2 - r_y^2}{r^2}\left[\frac{1}{2} + \frac{\mathrm{e}^{-r}(r^2+3r+3)-3}{r^2}\right] - \mathrm{Ei}(-r) + \ln r + \mathrm{e}^{-r} - 1 + E\right\}, \tag{4.3}$$

where r_x and r_y are the Cartesian components of $\boldsymbol{r} = \boldsymbol{x} - \boldsymbol{y}$, $r = |\boldsymbol{r}|$ and $E = 0.577\ldots$ is the Euler constant. Substitution of $c_{Y\phi}$ from (4.2) and γ_ϕ from (4.3) into the expression for u_{jk} in (3.13), followed by integration with $x_0 = y_0 = 0$ at $t_0 = 0$ in (3.20), yields the following expressions for the displacement covariances:

$$X_{12} = 0, \tag{4.4}$$

$$X_{11}(t) = \sigma_Y^2 \left\{2t - 3\ln t + \tfrac{3}{2} - 3E + 3\left[\mathrm{Ei}(-t) + \frac{\mathrm{e}^{-t}(1+t)}{t} - \frac{1}{t^2}\right]\right\}, \tag{4.5}$$

$$X_{22}(t) = \sigma_Y^2 \left\{\ln t - \tfrac{3}{2} + E - \mathrm{Ei}(-t) + 3\left[\frac{1}{t^2} - \frac{\mathrm{e}^{-t}(1+t)}{t}\right]\right\}. \tag{4.6}$$

Equations (4.5) and (4.6) have been obtained previously by a somewhat-different approach (Dagan 1982*b*), and they are represented graphically in figure 1 (*a*). As one would expect from Taylor's (1921) theory, in the small-time limit we get in (4.5) and (4.6)

$$X_{11}(t) \to \tfrac{3}{8}\sigma_Y^2 t^2, \quad X_{22}(t) \to \tfrac{1}{8}\sigma_Y^2 t^2 \quad (t \to 0). \tag{4.7}$$

Thus the covariance tensor is anisotropic, its longitudinal component being initially three times larger than the lateral one.

The more interesting limit is that of large t. Then we obtain in (4.5) and (4.6)

$$X_{11}(t) \to \sigma_Y^2(2t - 3\ln t + \tfrac{3}{2} - 3E + \ldots), \quad X_{22}(t) \to \sigma_Y^2(\ln t + E - \tfrac{3}{2} + \ldots) \quad (t \to \infty). \tag{4.8}$$

It is seen that the behaviour at large t is quite different from that at small t. $X_{11}(t)$ has the structure predicted by the Taylor theory, namely the leading term is proportional to t. Rewriting X_{11} in terms of variables with dimensions gives, in (4.8), $X_{11}(t) \to 2\sigma_Y^2 l_Y t$. In contrast, X_{22} grows only logarithmically with time, the reason being that u_{22} (3.13) has a zero integral scale. In figure 1 (*b*) we have represented the ratios $X_{11}/2t$ and $X_{22}/2t$ as functions of time. The significance of these quantities when interpreting field tests will be discussed in the sequel. In a similar fashion we could derive the coefficients D_{tjk} of (3.15) by differentiation of (4.5) and (4.6).

One of the most important conclusions that can be drawn from the inspection of figures 1 (*a*,*b*) is that $D_{jk} = \frac{1}{2}\mathrm{d}X_{jk}/\mathrm{d}t$ vary with time over a period which can be quite large. Thus D_{11} reaches its constant, asymptotic value only after a travel time equal to tens of conductivity integral scales over the average velocity.

Similar computations can be carried out for the three-dimensional covariance tensor $X_{jk}(t)$. The three components different from zero are now the longitudinal one X_{11} and the two lateral ones $X_{22}(t) = X_{33}(t)$. X_{11} and X_{22} are given by formulae similar to (4.5) and (4.6) respectively, the difference being that C_Y and G are now functions of the additional space variable z and an additional integration over z is carried out. The final result is now

$$X_{11}(t) = 2\sigma_Y^2\left[t - \frac{8}{3} + \frac{4}{t} - \frac{8}{t^3} + \frac{8}{t^2}\left(1 + \frac{1}{t}\right)\mathrm{e}^{-t}\right], \tag{4.9}$$

$$X_{22}(t) = X_{33}(t) = 2\sigma_Y^2\left[\frac{1}{3} - \frac{1}{t} + \frac{4}{t^3} - \left(\frac{4}{t^3} + \frac{4}{t^2} + \frac{1}{t}\right)\mathrm{e}^{-t}\right]. \tag{4.10}$$

The small- and large-time limits are given now by

$$X_{11}(t) \to \tfrac{8}{15}\sigma_Y^2 t^2, \quad X_{22}(t) \to \tfrac{1}{15}\sigma_Y^2 t^2 \quad (t \to 0), \tag{4.11}$$

$$X_{11}(t) \to \sigma_Y^2(2t - \tfrac{8}{3} + \ldots), \quad X_{22}(t) \to \sigma_Y^2\left(\frac{2}{3} - \frac{2}{t} + \ldots\right) \quad (t \to \infty), \tag{4.12}$$

and it is seen that the lateral covariances are much smaller than the longitudinal one. X_{11}/σ_Y^2 (4.9) and X_{22}/σ_Y^2 (4.10) are represented in figure 1 (*a*), whereas the ratios $X_{11}/2\sigma_Y^2 t$ and $X_{22}/2\sigma_Y^2 t$ are represented in figure 1 (*b*). It is seen that the lateral covariance (with dimensions) tends asymptotically to the constant value $\frac{2}{3}\sigma_Y^2 l_Y^2$.

To illustrate the results further, we shall now analyse an elaborate field experiment carried out recently by Sudicky, Cherry & Frind (1980). The results here are taken from the summary of the data presented by Simmons (1982). The test was performed for natural flowing conditions in a landfill by injecting a chloride solute through five pipewells, which established an initial parallelepipedic solute body. The concentration distribution in space was monitored subsequent to the injection of the solute body

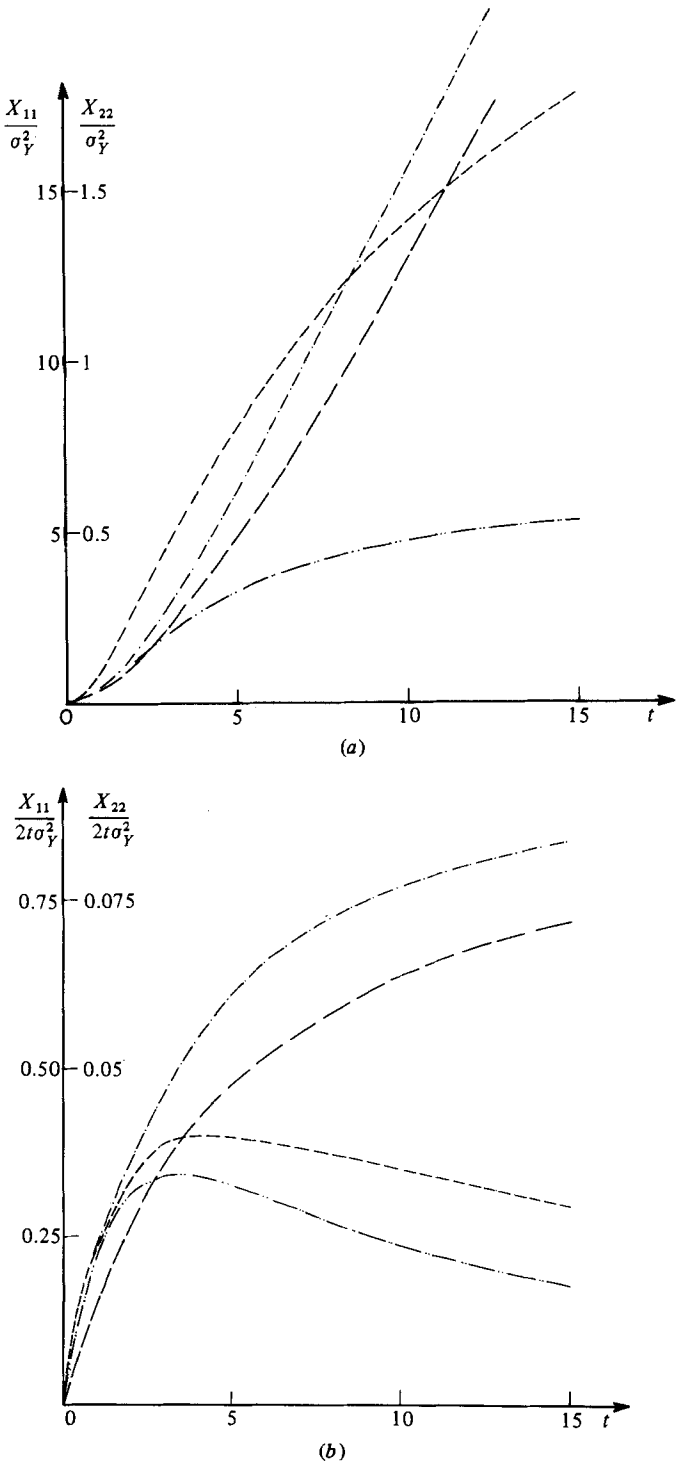

FIGURE 1. The displacement covariances as functions of time. (*a*) ———, X_{11}/σ_Y^2, two-dimensional flow (4.5); –·–·–·–, X_{11}/σ_Y^2, three-dimensional flow (4.9); – – –, X_{22}/σ_Y^2, two-dimensional flow (4.6); –··–··–, X_{22}/σ_Y^2, three-dimensional flow (4.10). (*b*) The same as in (*a*) after division by $2t$. Here and in the following figures, X_{11}, X_{22} are made dimensionless with respect to l_Y^2, and t with respect to l_Y/U.

by a battery of observation wells. The distance from the input zone was of the order of a few metres, i.e. the phenomenon was observed at the local scale. Unexpectedly, the tracer slug split into two halves that moved at different average velocities. Each half developed its own bell-shaped distribution and was employed separately in order to determine dispersion coefficients. We shall refer here to the results pertinent to the 'fast zone', those for the other half being similar.

The interpretation of the measurements was carried out by assuming that the concentration obeys the convection–diffusion equation with constant velocity and dispersion coefficient. The first was determined from the motion of the centre of gravity of the solute body. With the initial dimensions of the slug of 1.4 m × 2.25 m × 0.5 m, the dispersion coefficient at a certain location was determined by a best fit between the solution of the diffusion equation and measurements. The dispersivities were subsequently derived by dividing the dispersion coefficients by the velocity. It was found that dispersion in the vertical direction was exceedingly small and the tracer spread essentially in the horizontal plane. The experimental values of dispersivity as function of distance from the input zone are reproduced from Simmons (1982) in figure 2. The longitudinal and lateral pore-scale dispersivities were determined from the intercepts of the dispersivity curves at $x = 0$, where x is the longitudinal coordinate. The values are, in the notation of §3 and for dimensional variables, $D_{d11} = 0.011$ m and $D_{d22} = 0.0033$ m respectively.

Inspection of figure 2 shows that both dispersivities grew with distance from the input zone, i.e. with travel time, contrary to the assmption underlying the interpretation of results. This discrepancy was attributed to larger-scale heterogeneity of the porous formation. We shall try to analyse the experimental results by using the present developments.

We shall assume at present that the ergodic hypothesis is satisfied, i.e. that the space-averaged concentration along the measuring observation wells is equal to the concentration expectation value. This is a fundamental assumption which should not be taken for granted, but a thorough discussion of its applicability is deferred to §6. The next assumption is that transport is two-dimensional in the horizontal plane. Finally, we presume that the other conditions underlying the analytical expressions of the displacement covariances X_{11} (4.5) and X_{22} (4.6) are met.

The comparison between experiments and theory has been carried out as follows. The experimental concentration was assumed to be Gaussian, as is the case for the theoretical one. The connection between the time-dependent covariances X_{jk} and the constant dispersivities measured from a space concentration distribution at a given time is quite simple: the latter are obtained from the former by division by twice the velocity times the travel time (see (3.21)). The same result is approximately valid for measurement of time-dependent concentration at a fixed point. In other words, the curves representing $X_{jk}(t)/2t$ of figure 1 (*b*) are approximately those of the apparent dimensionless dispersivities in a common interpretation of field tests. Since everything is known except for the two parameters σ_Y^2 and l_Y, the variance and integral scale respectively of the log of the hydraulic conductivity, the two have been determined by a best fit of the theoretical curves of figure 1 (*a*) for two-dimensional flow and the measured values. The results are shown in figure 2 after finding the values $\sigma_Y^2 = 0.19$ and $l_Y = 1.4$ m. Of course, a better verification of the theory could be achieved by measuring these two parameters independently, but such data are difficult to obtain and unfortunately are not available. It is still encouraging to find out that in spite of the numerous simplifying assumptions, the theory is able to reproduce quite accurately the measured apparent dispersivities, and particularly the

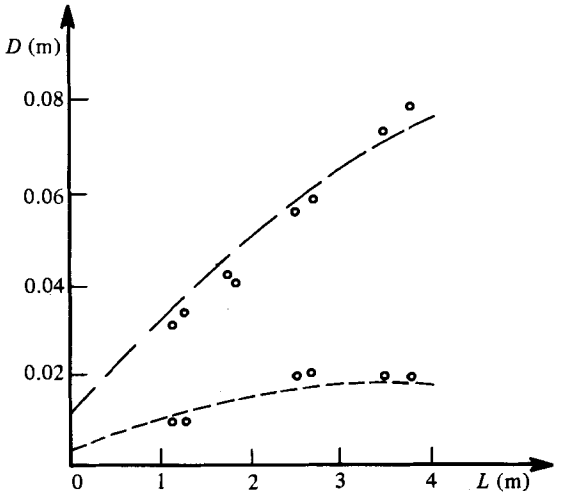

FIGURE 2. Comparison between experimental points from the field test of Sudicky *et al.* (1980) (reproduced from Simmons 1982) and theoretical curves (4.5, 4.6 and figure 1*b*) with $\sigma_Y^2 = 0.19$, $l_Y = 1.4$ m. D is the apparent longitudinal (———) and lateral (– – – –) dispersivity and $L = Ut$ is the distance travelled by the solute body.

relative magnitude of the two components, as well as their growth with time. It is hoped that further elaborate time-consuming and costly field experiments will become available for further validation and improvement of the theoretical analysis. At any rate, the values of σ_Y^2 and l_Y are of the order of magnitude implied by the approximations adopted in the preceding sections.

5. Brief discussion of previous work

The review of previous work on stochastic modelling of transport in porous formations has been deferred to this section to take advantage of the developments of the preceding sections. As a rule, the ergodic hypothesis has been adopted in the past and the computations have been limited to evaluating only the concentration expectation value.

The pioneering work of Buyevich, Leonov & Safrai (1969) assumes that heterogeneity is associated with the spatial variability of porosity, the permeability being a function of the latter. By adopting the linearized approximation and a spectral representation, these authors derived the spectral densities of the pressure, velocity and concentration fields. The results are quite involved because the Darcy law (3.1) has been replaced by a general momentum equation which contains various derivatives of the velocity field. In the final results on transport Buyevich *et al.* (1969) adopt a Gaussian isotropic porosity covariance function and derive the small- and large-time limits of the effective dispersion coefficents D_{ijk} (3.26).

A similar approach has been employed by Gelhar & Axness (1983), who related transport to spatial variability of hydraulic conductivity. They have evaluated only the asymptotic, constant, values of the dispersion coefficients D_{ijk} for large time and for various types of isotropic and nonisotropic log-conductivity covariances. The authors retain in the analysis both first-order convective velocities and pore-scale dispersion. This is tantamount in the present context to replacing $\boldsymbol{X}_t$ in (3.16) by $\langle \boldsymbol{X} \rangle + \boldsymbol{X}_d$ rather than by $\langle \boldsymbol{X} \rangle$ (3.17) only. In this respect their analysis is more general

than the present one, as D_{tjk} depend on terms of order $\sigma_Y^2 D_d$, which were neglected here. It is therefore instructive to compare the present results with the complementary ones of Gelhar & Axness (1983).

As expected, the values of the longitudinal component $D_{11} = \frac{1}{2}\mathrm{d}X_{11}/\mathrm{d}t$ for $t \to \infty$ obtained here by differentiating (4.5) and (4.9) are identical with the leading-order terms derived by Gelhar & Axness (1983, equations (3.3) and (3.7)) for the same correlation function (4.1). Thus their results are particular cases of those derived here. In contrast, they obtain finite limits for $D_{22} = \frac{1}{2}\mathrm{d}X_{22}/\mathrm{d}t$ for $t \to \infty$, namely $D_{22} = \frac{1}{15}\sigma_Y^2 D_{d11}$ for 3-dimensional flow (their equation (3.6)) and $D_{22} = \frac{1}{8}\sigma_Y^2 D_{d11}$ (their equation (3.7)) for 2-dimensional flow. These results may be used in order to delimit the range of validity of the time-dependent X_{22} (4.6, 4.10). It is seen that for two-dimensional flow the approximation (4.6), in which the interaction between heterogeneity and pore-scale dispersion is neglected, is valid for $t \ll 4/D_{d11}$, whereas for 3-dimensional flow X_{22} (4.10) is valid for $t \ll \frac{1}{3}D_{d11}^{-1}$. Since D_{d11}, the ratio between pore-scale or local dispersivity and the integral scale l_Y, is much smaller than unity, the expressions derived here are uniform approximations for travel distances of many integral scales. It will be of interest, nevertheless, to derive uniformly valid time-dependent expressions for X_{22} along the lines of Gelhar & Axness' (1983) approach.

Mathèron & de Marsily (1980) have investigated transport in a formation made up from parallel layers set at random, such that the hydraulic conductivity is a function of one space coordinate only, normal to the layer planes. In contrast with the previous works, they have been able to derive expressions for the dispersion coefficients for arbitrarily large covariances. The main result was that for flow parallel to the layers the longitudinal dispersion coefficient does not tend to a finite limit for $t \to \infty$. A similar case of stratified aquifer, but of finite thickness, has been investigated by Gelhar, Gutjahr & Naff (1979).

Finally, Smith & Schwartz (1980) have carried out a numerical simulation of two-dimensional flow and of transport by using a Monte Carlo procedure. Their results, which are not limited by small variances and do not imply ergodicity, show clearly that the expectation concentration does not generally satisfy a dispersion equation. Because of numerical complexity, however, their study has been confined to some particular cases solely.

6. The concentration variance and the ergodic hypothesis

We consider now the concentration field associated with a solute body inserted at $t = 0$ into a volume V_0. Furthermore, the concentration is space-averaged over a fixed volume V surrounding a point of coordinate $\boldsymbol{x}$. To simplify matters the initial concentration is assumed to be constant i.e. $C(\boldsymbol{x}_0, 0) = C_0$. Then, by using (3.14), we can write the concentration as

$$\bar{C}(\boldsymbol{x}, t) = \frac{1}{V}\int_V C(\boldsymbol{x}', t)\,\mathrm{d}\boldsymbol{x}' = \frac{C_0}{V}\int_V \int_{V_0} \delta[\boldsymbol{x}' - \boldsymbol{X}_t(t; \boldsymbol{x}_0, 0)]\,\mathrm{d}\boldsymbol{x}_0\,\mathrm{d}\boldsymbol{x}'. \tag{6.1}$$

We define now the joint p.d.f. of two displacements $\boldsymbol{X}_t(t, \boldsymbol{a})$ and $\boldsymbol{Y}_t(t, \boldsymbol{b})$ of two particles originating at $t = 0$ from $\boldsymbol{x}_0 = \boldsymbol{a}$ and $\boldsymbol{x}_0 = \boldsymbol{b}$ respectively. The displacements are decomposed as in (3.15), i.e. $\boldsymbol{X}_t = \boldsymbol{X} + \boldsymbol{X}_d$ and $\boldsymbol{Y}_t = \boldsymbol{Y} + \boldsymbol{Y}_d$. The 'Brownian-motion' components are uncorrelated if $\boldsymbol{a} \neq \boldsymbol{b}$, which is an approximation reflecting the smallness of their correlation scale as compared with that of the convective components $\boldsymbol{X}$ and $\boldsymbol{Y}$. For average uniform flow, the latter are related to the Eulerian

steady velocity field by (3.16) with $\boldsymbol{x}_0$ replaced by $\boldsymbol{a}$ and $\boldsymbol{b}$ respectively and with $t_0 = 0$. Finally, under the same conditions of a first-order approximation of the velocity and concentration fields, the fluctuations $\boldsymbol{X}'$ and $\boldsymbol{Y}'$ are given by (3.18) with $\boldsymbol{x}_0 = \boldsymbol{a}, \boldsymbol{b}$. Hence, owing to the normality of $\boldsymbol{u}$, $\boldsymbol{X}$ and $\boldsymbol{Y}$ are also normal and their joint p.d.f. $f(\boldsymbol{X}, \boldsymbol{Y}; t, \boldsymbol{a}, \boldsymbol{b})$ is given by an expression similar to (3.19) with X_{jk} replaced by the covariance tensor $Z_{XY,jk}$, which is symmetrical and has 36 or 16 components in the three- or two-dimensional cases respectively.

The covariance tensor is related to the velocity covariance by relationships similar to (3.20) as follows:

$$Z_{XY,jk} = \int_0^t \int_0^t u_{jk}(a_1 + t', a_2, a_3, b_1 + t', b_2, b_3)\, \mathrm{d}t'\, \mathrm{d}t''. \tag{6.2}$$

For the case of statistical homogeneity considered in this part, the mixed components of the covariance tensor are functions only of the initial space lag $\boldsymbol{a} - \boldsymbol{b}$ between the two particles, i.e.

$$Z_{XY,jk}(t, \boldsymbol{a} - \boldsymbol{b}) = \int_0^t \int_0^t u_{jk}(a_1 - b_1 + t' - t'', a_2 - b_2, a_3 - b_3)\, \mathrm{d}t'\, \mathrm{d}t'' \quad (\boldsymbol{X} \neq \boldsymbol{Y}), \tag{6.3}$$

whereas those related to the same particle are given by

$$Z_{XX,jk}(t) = Z_{YY,jk}(t) = X_{jk}(t) \quad (\boldsymbol{X} \equiv \boldsymbol{Y}). \tag{6.4}$$

Finally, the covariance of the total displacements is given by

$$\left.\begin{aligned} Z_{tjk} &= Z_{XY,jk} \quad (\boldsymbol{X} \neq \boldsymbol{Y}), \\ Z_{tjk} &= X_{jk} + 2D_{djk}t \quad (\boldsymbol{X} = \boldsymbol{Y}). \end{aligned}\right\} \tag{6.5}$$

We proceed now with the main topic of this section, namely the computation of the concentration variance (we could, of course, evaluate other moments as well). This is achieved immediately by ensemble-averaging $\bar{C}^2$ (6.1) and subtracting $\langle \bar{C} \rangle^2$ from it. The important result is

$$\sigma_{\bar{C}}^2(\boldsymbol{x}, t) = \frac{C_0^2}{V^2} \int_{V_0} \int_{V_0} \int_V \int_V [f_t(\boldsymbol{X}, \boldsymbol{Y}, t; \boldsymbol{a}, \boldsymbol{b}) - f_t(\boldsymbol{X}, t; \boldsymbol{a}) f_t(\boldsymbol{Y}t; \boldsymbol{b})]\, \mathrm{d}\boldsymbol{X}\, \mathrm{d}\boldsymbol{Y}\, \mathrm{d}\boldsymbol{a}\, \mathrm{d}\boldsymbol{b}, \tag{6.6}$$

where $f_t(\boldsymbol{X}, \boldsymbol{Y}, t; \boldsymbol{a}, \boldsymbol{b})$ is the normal distribution of covariance Z_{tjk}, whereas $f_t(\boldsymbol{X}, t)$ has covariance X_{tjk} (3.22) and the averages of $\boldsymbol{X}_t$ and $\boldsymbol{Y}_t$ are given by (3.17), i.e. $\langle \boldsymbol{X}_t \rangle = \boldsymbol{a} + t\boldsymbol{i}$ and $\langle \boldsymbol{Y}_t \rangle = \boldsymbol{b} + t\boldsymbol{i}$.

It is seen that the concentration variance depends in the displacement covariance (6.3). Once the latter is known $\sigma_{\bar{C}}^2$ can be found by a series of quadratures over the normal distribution. Before proceeding with the derivation of $Z_{XY,jk}$ we shall analyse first in a qualitative manner the dependence of $\sigma_{\bar{C}}^2$ upon the extent of V_0 or V.

Since the velocity components become uncorrelated for sufficiently large initial lag $\boldsymbol{a} - \boldsymbol{b}$, the same will be shown to be true for the corresponding displacements, and $Z_{XY,jk}$ tend to zero for fixed t and sufficiently large $h = |\boldsymbol{a} - \boldsymbol{b}|$. For such lags $\boldsymbol{X}_t$ and $\boldsymbol{Y}_t$ become statistically independent and $f_t(\boldsymbol{X}, \boldsymbol{Y}, t; \boldsymbol{a}, \boldsymbol{b}) \to f_t(\boldsymbol{X}, t; \boldsymbol{a}) f_t(\boldsymbol{Y}, t; \boldsymbol{b})$. Then by (6.6) the concentration coefficient of variation tends to zero if the lengthscales of V_0 or V are sufficiently large compared with the correlation scale l_Y. Assuming that the same is true for the higher-order statistical moments of C, the actual concentration is close to its expectation value and the requirements of the ergodic hypothesis are fulfilled. It should be emphasized that, unlike turbulent or other flows fluctuating in time, in the case of steady flow through a medium of fixed random structure, continuous insertion of the solute over an extended period of time has no effect upon the reduction of variance. In simple words, parcels of tagged fluid injected at different

times in the formation will follow the same path, and ergodicity can be achieved either if V_0 or V are sufficiently large, or after an exceedingly large travel time for which the dispersive effect of the 'Brownian-motion' component ensures spreading over a large volume.

The salient question is whether in typical applications of solute transport in porous formations the above ergodicity requirements are satisfied. The point of view expressed already in a previous work (Dagan 1982*b*) is that in the case of spreading at the local scale the answer is positive, whereas for transport at regional scale it is generally negative. Indeed, in most cases of field experiments at the local scale, solute is introduced either through an injecting well or a repository. In any case the lengthscale of the initial solute body is relatively large compared with the heterogeneity correlation scale, and this was precisely the case in the example analysed in §4. The concentration is generally measured with the aid of piezometers, which achieve a space averaging over a vertical scale which might be comparable to l_Y. Although the computational tools needed in order to check this assertion quantitatively are at hand, we shall take for granted here that in most circumstances it is satisfied.

The situation is generally different for transport at regional scale. In this case, one is interested in the fate of the solute body at distances of the order of kilometres from the input zone, and the transmissivity correlation scale in the plane is of the order of hundreds or thousands of metres (see §2). Only in the case of distributed sources over large areas, of the order of kilometres, is one entitled to assume ergodicity. In many conceivable cases of local sources, the initial lengthscale is small compared with the regional scale, and the concentration variance can be quite large. The smoothing effect of space averaging is also of limited scope, since again one is generally interested in the fate of solutes over zones of small extent. Most of the developments in the sequel are dedicated therefore to two-dimensional solute transport under conditions of possibly large concentration coefficient of variation.

At this point we return to the evaluation of the covariance tensor $Z_{XY,jk}$ (6.3) in two dimensions for the particular c_Y (4.1). This could be done in a closed analytical form by using the functions $c_{Y\phi}$ (4.2) and γ_ϕ (4.3).

The cross-component $Z_{XY,12}$ is equal to zero for both $h = 0$ and $h \to \infty$, and is negligible. Hence the tensor $Z_{XY,jk}$ $(j, k = 1, 2)$ is symmetrical and has zero components for $j \neq k$, and the surviving components are $Z_{XX,11} = Z_{YY,11} = X_{11}(t)$ (4.5), $Z_{XX,22} = Z_{YY,22} = X_{22}(t)$ (4.6), $Z_{XY,11} = Z_{YX,22}$ and $Z_{XY,22} = Z_{YX,22}$ (6.3).

We have represented in figure 3 the dependence of $Z_{XY,jk}$ upon t for a few values of the initial lags h_x and h_y. Examination of figure 3 shows that the covariance of longitudinal displacements drops from X_{11} to zero as the lateral lag h_y increases from 0 to 3, whereas that of the lateral displacements is reduced to half of X_{22} under the same conditions. In contrast, the longitudinal initial lag h_x has a small influence upon the covariances, i.e. the displacements of two particles lying on a line parallel to the mean flow remain correlated for large separations.

We can conclude from the results of figure 3 that, for an input zone extending a few correlation scales l_Y across the direction of the mean flow, the concentration coefficient of variation becomes small and the expectation value is close to the space average, the latter being taken over a volume which might be small at the transmissivity correlation scale. This conclusion is valid for the dimensionless time interval of say $t < 30$. Different conclusions could be reached for very large t when the local scale dispersivity ensures spreading over a large volume, but they are of little interest for applications related to regional scale.

In contrast, for an input zone V_0 of transversal dimension smaller than say $h_y = 0.2$,

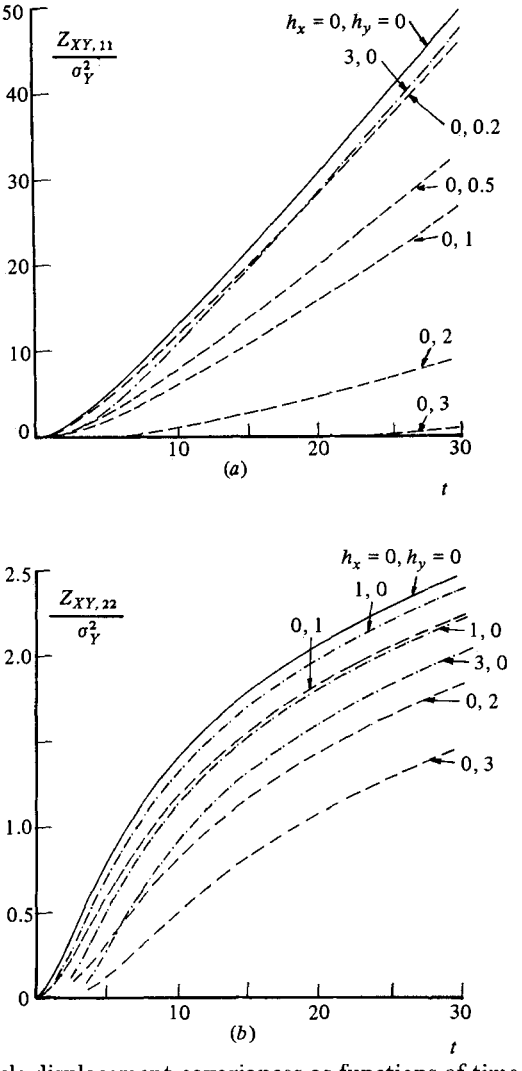

FIGURE 3. The two-particle displacement covariances as functions of time for two-dimensional flow for various initial distances $\boldsymbol{h}(h_x, h_y)$ between particles.

the covariances $Z_{XY,11}$ and $Z_{XY,22}$ are close to X_{11} and X_{22} respectively, and the coefficient of variation may be quite large. Indeed, the two particles covariances (6.3) are approximately equal to

$$\left.\begin{aligned} Z_{tjk} = Z_{XY,jk} = X_{jk} \quad (\boldsymbol{X} \neq \boldsymbol{Y},\ j = k), \\ Z_{tjk} = X_{tjk} = X_{jk} + 2D_{djk}t \quad (\boldsymbol{X} \equiv \boldsymbol{Y};\ j = k), \end{aligned}\right\} \tag{6.7}$$

where we have assumed that $\boldsymbol{a}-\boldsymbol{b}$ is sufficiently small to warrant its neglect in $Z_{XY,jj}$, but sufficiently large to permit one to discard the 'Brownian-motion' component when $\boldsymbol{a} \neq \boldsymbol{b}$. Under these conditions of small V_0 and V at scale l_Y it can be shown that for dimensionless time in the range of $(a_2-b_2)^2/D_{d22} \ll t \ll D_{d22}^{-2}$ the covariance and expectation value have the simple expressions

$$\left.\begin{aligned} \sigma_{\bar{C}}^2(\boldsymbol{x}, t) = C_0^2\, V_0^2\, [f_t(\boldsymbol{x}, \boldsymbol{x}, t; \boldsymbol{a}, \boldsymbol{a}) - f_t^2(\boldsymbol{x}, t; \boldsymbol{a})], \\ \langle \bar{C} \rangle \approx C_0\, V_0 f_t(\boldsymbol{x}, t; \boldsymbol{a}). \end{aligned}\right\} \tag{6.8}$$

The computation of the coefficient of variation $\epsilon_{\bar{C}}$ can be carried out easily by using the multivariate normal distribution f_t with covariance (6.7). Thus, at the 'centre of gravity' of $\langle \bar{C} \rangle$, at $x = a_1 + t$, $y = a_2$, the coefficient of variation attains its minimal value, which is given by

$$\epsilon_{\bar{C}}(t + a_1, a_2, t) = \left[\frac{(X_{11} X_{22})^{\frac{1}{2}}}{4(D_{d11} D_{d22})^{\frac{1}{2}} t} - 1 \right]^{\frac{1}{2}}. \tag{6.9}$$

To grasp the order of magnitude of $\epsilon_{\bar{C}}$ let us take $t = 10$, $X_{11} = 13$ (figure 1*a*), $X_{22} = 1.4$ (figure 1*a*), $D_{d11} = 0.1$ and $D_{d22} = 0.01$. For these values we obtain in (6.9) $\epsilon_{\bar{C}} = 3.1$. This is a large value, which implies that the actual concentration in a given realization may differ considerably from its expectation value, and the concentration is subjected to a large degree of uncertainty.

7. Summary of Part 1

Summarizing the main results of this part, we suggest the following picture for solute transport in heterogeneous formations. (i) For input zones V_0 and space averaging volumes V larger than the log-conductivity integral scale l_Y the transport at local scale can be described by the dispersion-type equation (3.25), obeyed by the concentration expectation value. The dispersion coefficients depend on the travel time, as illustrated in figure 1 for an exponential log-conductivity autocovariance. Only after a travel distance of tens of integral scales do the dispersivities tend to the asymptotic constant limits derived approximately here or by Gelhar & Axness (1983) for small σ_Y^2. (ii) In the case of transport at regional scale and for input zones and averaging areas much smaller than the log-transmissivity scale, as is the case in most applications of 'point sources', the concentration is subjected to a large degree of uncertainty. The computation of the concentration expectation value is of little use and the coefficients appearing in the right-hand side of (3.25) cannot be interpreted as effective dispersion coefficients, unless a considerable travel time has elapsed. We can picture a solute plume in a given realization as diffusing slowly owing to local scale dispersion and winding like a meandering stream because of large-scale regional heterogeneity. In the set of various possible realizations underlying the calculation of the concentration statistical moments, the location of the plume may differ considerably from the actual one, which is precisely reflected by the large value of the concentration coefficient of variation.

An obvious way to eliminate uncertainty is to regard the large-scale motion as deterministic. However, this requires detailed information about the spatial distribution of the conductivity at regional scale, and such information is generally available only at a few points of the formation. In the second part of the study we show how uncertainty can be reduced by using such field measurements of formation and flow parameters.

PART 2. INFLUENCE OF HEAD AND CONDUCTIVITY CONDITIONING UPON CONCENTRATION FIELD

8. Effect of conditioning upon the transmissivity and head fields

In the present part we shall deal exclusively with two-dimensional flow at the regional scale, although the approach outlined here is of general applicability.

In Part 1 we have assumed that the only information available on the formation random structure is the mean m_Y and the covariance $C_Y(\boldsymbol{r})$ of the log conductivity Y, which is multivariate normal. In practice these parameters are derived from field data, i.e. by measuring Y at a set of points $\boldsymbol{x}_j$ ($j = 1, \ldots, M$) and carrying out statistical analysis, and in §2 we have mentioned a few published studies on particular formations. By making use of the mean and covariance only, we assume that Y is subjected to some degree of uncertainty at each point and we ignore the fact that, at the points of coordinates $\boldsymbol{x}_j$, Y is known deterministically, or within measurement errors. Here again it is worthwhile to emphasize the difference between a fixed random structure and a time-fluctuating field. In the first case, measurements that were carried out once can be used at any instant to characterize the structure.

The main aim of the present part of the study is to investigate the impact of measured formation and flow data upon the concentration field. The only known previous work on the subject is that of Smith & Schwartz (1980), who have examined, by Monte Carlo numerical simulations, the influence of fixing the conductivity at a few points in particular cases of flow. Devary & Doctor (1982) have analysed a few covariances of flow variables as a preparatory step towards modelling of solute transport.

We shall consider here two types of measurements, which differ in methodology and impact. The first one, already mentioned, is that of transmissivity, i.e. of Y, which is generally carried out by pumping tests. Such a test provides data on the formation structure and can be used for modelling and prediction of flow under various boundary conditions, but is quite costly. The second one is measurement of head Φ by using piezometers, which is much simpler, but provides data on the actual flow conditions only.

Incorporation of data at fixed points in the statistics of a random function of spatial coordinates has been dealt with extensively in geostatistics (see e.g. Journel & Huijbregts 1978). One of the basic problems approached in geostatistics is that of stochastic interpolation, which is solved by the method of kriging. The latter uses a linear interpolator in order to predict the conditioned expectation value and covariance on the basis of the unconditioned covariance. We shall follow here a different approach outlined in a previous work (Dagan 1982*a*), which leads to similar results and is based on elementary statistics. For the sake of completeness, we outline the procedure briefly here.

Consider the log-conductivity fluctuation $Y'(\boldsymbol{x}) = Y(\boldsymbol{x}) - m_Y$, which is supposed to be stationary and normal, and defined therefore by the covariance $C_Y(\boldsymbol{x}, \boldsymbol{x}')$. Assume now that $Y'_j = Y'(\boldsymbol{x}_j)$ ($j = 1, \ldots, M$) and $\phi_k = \phi(\boldsymbol{x}_k)$ ($k = M+1, \ldots, N$) are measured values of Y' at M points and of the head fluctation ϕ at $N-M$ points respectively. This information is taken into account by defining the conditional probability density function of Y' on the subset of realizations in which Y'_j and ϕ_k are fixed and given. The derivation of the conditional binormal p.d.f. of $Y'(\boldsymbol{x})$ and $Y'(\boldsymbol{x}')$ may be found in textbooks (e.g. Mood & Graybill 1963, §9.3). Thus the conditional expectation value $m_Y^c(\boldsymbol{x})$ and the conditional covariance $C_Y^c(\boldsymbol{x}, \boldsymbol{x}')$ are given by

$$m_Y^c(\boldsymbol{x}) = \sum_{j=1}^{M} \lambda_j(\boldsymbol{x})\, Y'_j + \sum_{k=M+1}^{N} \mu_k(\boldsymbol{x})\, \phi_k, \tag{8.1}$$

$$C_Y^c(\boldsymbol{x}, \boldsymbol{x}') = C_Y(\boldsymbol{x}, \boldsymbol{x}') - \sum_{j=1}^{M} \lambda_j(\boldsymbol{x})\, C_Y(\boldsymbol{x}', \boldsymbol{x}_j) - \sum_{k=M+1}^{N} \mu_k(\boldsymbol{x})\, C_{Y\phi}(\boldsymbol{x}', \boldsymbol{x}_k), \tag{8.2}$$

where the coefficients λ_j and μ_k are solutions of the linear system

$$\left.\begin{aligned} &\sum_{j=1}^{M} \lambda_j C_Y(\boldsymbol{x}_j, \boldsymbol{x}_l) + \sum_{k=M+1}^{N} \mu_k C_{Y\phi}(\boldsymbol{x}_j, \boldsymbol{x}_k) = C_Y(\boldsymbol{x}, \boldsymbol{x}_l) \quad (l = 1, \ldots, M), \\ &\sum_{j=1}^{M} \lambda_j C_{Y\phi}(\boldsymbol{x}_j, \boldsymbol{x}_l) + \sum_{k=M+1}^{N} \mu_k C_{\phi}(\boldsymbol{x}_j, \boldsymbol{x}_k) = C_{Y\phi}(\boldsymbol{x}, \boldsymbol{x}_l) \quad (l = M+1, \ldots, N). \end{aligned}\right\} \tag{8.3}$$

In these equations $C_{Y\phi}$ and C_Y are unconditional covariances (see 3.4). In the present case the standard system (8.3) needs to be slightly generalized because the head variance σ_ϕ^2 becomes unbounded for two-dimensional flow in an infinite domain (§3). This difficulty is easily circumvented by a procedure suggested in a previous work (Dagan 1982*a*) and in §3, by substituting $C_\phi = \sigma_\phi^2 - \Gamma_\phi$ in (8.3) and taking the limit $\sigma_\phi^2 \to \infty$.

The resulting linear system which replaces (8.3) is now

$$\left.\begin{aligned} &\sum_{j=1}^{M} \lambda_j C_Y(\boldsymbol{x}_j, \boldsymbol{x}_l) + \sum_{k=M+1}^{N} \mu_k C_{Y\phi}(\boldsymbol{x}_k, \boldsymbol{x}_l) = C_Y(\boldsymbol{x}, \boldsymbol{x}_l) \quad (l = 1, \ldots, M), \\ &\sum_{j=1}^{M} \lambda_j C_{Y\phi}(\boldsymbol{x}_j, \boldsymbol{x}_l) - \sum_{k=M+1}^{N} \mu_k \Lambda_\phi(\boldsymbol{x}_k, \boldsymbol{x}_l) + \Lambda(\boldsymbol{x}) = C_{Y\phi}(\boldsymbol{x}, \boldsymbol{x}_l) \quad (l = M+1, \ldots, N), \\ &\sum_{k=M+1}^{N} \mu_k = 0, \end{aligned}\right\} \tag{8.4}$$

giving λ_j, μ_k and Λ in terms of the unconditional variogram Γ_ϕ (3.10) rather than C_ϕ.

It is worthwhile to recall here a few properties of the conditional probability. (i) The bivariate normal p.d.f. of $Y'(\boldsymbol{x})$ and $Y'(\boldsymbol{x}')$ is not stationary, even if their unconditional p.d.f. is stationary. Indeed, the expectation value (8.1) depends on $\boldsymbol{x}$, whereas the covariance (8.2) depends on $\boldsymbol{x}$ and $\boldsymbol{x}'$ rather than on $\boldsymbol{x} - \boldsymbol{x}'$. (ii) The conditional variance $(\sigma_Y^2)^c = C_Y^c(\boldsymbol{x}, \boldsymbol{x})$ is smaller or equal to the unconditional, constant variance. In particular, the variance is zero at the points of conductivity conditioning and tends to the unconditional variance far from them. (iii) The conditional covariance does not depend on the actual measured values, but only on the unconditional covariance and the coordinates of the measurement points. (iv) For the first-order approximations of the unconditional covariances (3.5), the conditional covariance is also proportional to σ_Y^2, whereas the coefficents λ_j, μ_k and Λ are $O(1)$ and depend only on $\boldsymbol{x}_j$ and $\boldsymbol{x}_k$.

The conditional covariance $C_{Y\phi}^c(\boldsymbol{x}, \boldsymbol{x}')$ can be expressed with the aid of the same coefficients of (8.4) as

$$C_{Y\phi}^c(\boldsymbol{x}, \boldsymbol{x}') = C_{Y\phi}(\boldsymbol{x}, \boldsymbol{x}') - \sum_{j=1}^{M} \lambda_j(\boldsymbol{x})\, C_{\phi Y}(\boldsymbol{x}', \boldsymbol{x}_j) - \Lambda(\boldsymbol{x}) + \sum_{k=M+1}^{N} \mu_k(\boldsymbol{x})\, \Gamma_\phi(\boldsymbol{x}', \boldsymbol{x}_k). \tag{8.5}$$

Finally, by a similar procedure, the conditional mean and covariance of the head fluctuation are given by

$$m_\phi^c(\boldsymbol{x}) = \sum_{j=1}^{M} \lambda_j'(\boldsymbol{x})\, Y_j' + \sum_{k=M+1}^{N} \mu_k'(\boldsymbol{x})\, \phi_k, \tag{8.6}$$

$$C_\phi^c(\boldsymbol{x}, \boldsymbol{x}') = -\Gamma_\phi(\boldsymbol{x}, \boldsymbol{x}') - \sum_{j=1}^{M} \lambda_j'(\boldsymbol{x})\, C_{\phi Y}(\boldsymbol{x}', \boldsymbol{x}_j) - \Lambda'(\boldsymbol{x}) + \sum_{k=M+1}^{N} \mu_k'(\boldsymbol{x})\, \Gamma_\phi(\boldsymbol{x}', \boldsymbol{x}_k), \tag{8.7}$$

with λ'_j, μ'_k and Λ' solutions of

$$\left.\begin{aligned} &\sum_{j=1}^{M} \lambda'_j C_Y(\boldsymbol{x}_j, \boldsymbol{x}_l) + \sum_{k=M+1}^{N} \mu'_k C_{Y\phi}(\boldsymbol{x}_j, \boldsymbol{x}_l) = C_{\phi Y}(\boldsymbol{x}, \boldsymbol{x}_l) \quad (l = 1, \ldots, M), \\ &\sum_{j=1}^{M} \lambda'_j C_{Y\phi}(\boldsymbol{x}_j, \boldsymbol{x}_l) - \sum_{k=M+1}^{N} \mu'_k \Gamma_\phi(\boldsymbol{x}_k, \boldsymbol{x}_l) + \Lambda' = -\Gamma_\phi(\boldsymbol{x}, \boldsymbol{x}_l) \quad (l = M+1, \ldots, N), \\ &\sum_{k=M+1}^{N} \mu'_k = 1. \end{aligned}\right\} \tag{8.8}$$

If there is no head conditioning, $C^c_\phi(\boldsymbol{x}, \boldsymbol{x}')$ in (8.7) becomes unbounded. Then the conditional variogram is given by

$$\Gamma^c_\phi(\boldsymbol{x}, \boldsymbol{x}') = \Gamma_\phi(\boldsymbol{x}, \boldsymbol{x}') + \sum_{j=1}^{M} \lambda'_j(\boldsymbol{x})\, C_{\phi Y}(\boldsymbol{x}', \boldsymbol{x}_j), \tag{8.9}$$

replacing (8.7). These relationships summarize the material needed in the present study. Recall that the unconditional $C_{Y\phi}$ and Γ_ϕ depend on C_Y and have been given explicitly in (4.2) and (4.3) for the particular exponential covariance (4.1).

9. The influence of conditioning upon the velocity and concentration fields

Since the concentration is closely related to the velocity mean and covariances, we shall derive first their expressions under conditioning. The starting point is (3.12) for the velocity components, which are rewritten in the two-dimensional case as

$$U(\boldsymbol{x}) = 1 - u(\boldsymbol{x}), \quad u(\boldsymbol{x}) = Y'(\boldsymbol{x}) - \frac{\partial \phi(\boldsymbol{x})}{\partial x}, \quad v(\boldsymbol{x}) = -\frac{\partial \phi(\boldsymbol{x})}{\partial y}. \tag{9.1}$$

Equations (9.1) are assumed to be valid in both cases of conditional and unconditional probabilities, consistent with the relationship (3.7) adopted for the head ϕ. Furthermore, we adopt the first-order approximations for $C_{Y\phi}$ and Γ_ϕ (3.5, 3.8), which in turn are determined in an explicit form by C_Y. Consequently, the coefficients of (8.4) and (8.8), as well as the conditional mean and covariances of Y' and ϕ, are set. The velocity components in (9.1) are normal since they result from linear operations on Y' and their joint p.d.f. is entirely characterized by the mean and covariance. Thus the conditional expectation value is obtained by averaging (9.1) as follows:

$$\langle u^c(\boldsymbol{x}) \rangle = m^c_{Y'}(\boldsymbol{x}) - \frac{\partial m^c_\phi(\boldsymbol{x})}{\partial x}, \quad \langle v^c(\boldsymbol{x}) \rangle = -\frac{\partial m^c_\phi(\boldsymbol{x})}{\partial y}, \tag{9.2}$$

where $m^c_{Y'}(\boldsymbol{x})$ and $m^c_\phi(\boldsymbol{x})$ are given by (8.1) and (8.6) respectively. The spatial distribution of the conditional mean (9.2) depends ultimately on C_Y and on Y and ϕ measured values.

Similarly, the covariances are given in a general form by (3.13). In the notation of (9.1) and for conditional probability we have

$$u^c_{xx}(\boldsymbol{x}, \boldsymbol{x}') = C^c_Y(\boldsymbol{x}, \boldsymbol{x}') - \frac{\partial C^c_{Y\phi}(\boldsymbol{x}, \boldsymbol{x}')}{\partial x'} - \frac{\partial C^c_{Y\phi}(\boldsymbol{x}', \boldsymbol{x})}{\partial x} + \frac{\partial^2 C^c_\phi(\boldsymbol{x}, \boldsymbol{x}')}{\partial x\, \partial x'}, \tag{9.3}$$

$$u^c_{yy}(\boldsymbol{x}, \boldsymbol{x}') = \frac{\partial^2 C^c_\phi(\boldsymbol{x}, \boldsymbol{x}')}{\partial y\, \partial y'}, \quad u^c_{xy}(\boldsymbol{x}, \boldsymbol{x}') = -\frac{\partial C^c_{Y\phi}(\boldsymbol{x}, \boldsymbol{x}')}{\partial y'} + \frac{\partial^2 C^c_\phi(\boldsymbol{x}, \boldsymbol{x}')}{\partial x\, \partial y'}, \tag{9.4}$$

and they do not depend on the measured values, but only on $\boldsymbol{x}_j$ and $\boldsymbol{x}_k$.

The next step is the computation of the statistical moments of the particle

displacement $\boldsymbol{X}_t$, which is also normal. The conditional mean can be derived from the differential equation defining the trajectory:

$$\frac{\mathrm{d}\langle \boldsymbol{X}^c(t)\rangle}{\mathrm{d}t} = \boldsymbol{i} + \langle \boldsymbol{u}^c(\boldsymbol{X}_t^c)\rangle, \tag{9.5}$$

where we take, for the sake of simplicity, $t_0 = 0$, $\boldsymbol{x}_0 = 0$.

A first approximation of (9.5) is obtained by the same procedure as in §3 by replacing $\boldsymbol{X}_t^c$ in (9.5) by its average, the fluctuation $\boldsymbol{X}'^c$ being assumed to yield terms of higher order. Then (9.5) is replaced by

$$\frac{\mathrm{d}\langle \boldsymbol{X}^c(t)\rangle}{\mathrm{d}t} = \boldsymbol{i} + \langle \boldsymbol{u}^c(\langle \boldsymbol{X}^c\rangle)\rangle. \tag{9.6}$$

Equation (9.6) is a deterministic first-order differential system which in general can be integrated only numerically. The solution renders the streamlines of the steady average velocity field. A further simplification, consistent with the first-order perturbation approximation, is arrived at by replacing $\langle \boldsymbol{X}^c\rangle$ in (9.6) by its unconditional mean, i.e.

$$\langle \boldsymbol{X}^c(t)\rangle = t\boldsymbol{i} + \int_0^t \langle \boldsymbol{u}^c(t', 0)\rangle \, \mathrm{d}t', \tag{9.7}$$

leading to the mean trajectory in an explicit form. In any case, the effect of conditioning manifests in the departure of the latter from its straight-line unconditional mean (3.17). Furthermore, mean trajectories originating at different points are no more parallel owing to the dependence of $\langle \boldsymbol{u}^c\rangle$ upon the coordinates of the conditioning points.

The displacement covariances are computed by the same type of approximation as (3.20), i.e. by replacing $\boldsymbol{X}_t^c$ by $\langle \boldsymbol{X}^c\rangle$ in the Eulerian velocity covariances as follows:

$$X_{jk}^c(t) = \int_0^t \int_0^t u_{jk}^c[\langle \boldsymbol{X}^c(t')\rangle, \langle \boldsymbol{X}^c(t'')\rangle] \, \mathrm{d}t' \, \mathrm{d}t''. \tag{9.8}$$

Since the average displacement $\langle \boldsymbol{X}^c\rangle$ (9.6, 9.7) is not a simple function of t, generally the integration has to be performed numerically in (9.8). If $\langle \boldsymbol{X}^c\rangle$ does not depart too much from the unconditional straight mean path (3.17), a simple approximation of the covariances X_{jk}^c, which is consistent with the first-order solution, is obtained by replacing $\langle \boldsymbol{X}^c\rangle$ by $\langle \boldsymbol{X}\rangle = t\boldsymbol{i}$ in the integrand of (9.8), i.e.

$$X_{jk}^c(t) = \int_0^t \int_0^t u_{jk}^c(t', 0, t'', 0) \, \mathrm{d}t' \, \mathrm{d}t''. \tag{9.9}$$

Once X_{jk}^c is computed by integrating u_{jk}^c (9.8, 9.9), the Gaussian p.d.f. of $\boldsymbol{X}_t^c$ is precisely (3.19) in which $\langle \boldsymbol{X}\rangle$ and X_{jk} are replaced by $\langle \boldsymbol{X}^c\rangle$ (9.6 or 9.7) and $X_{jk}^c + 2D_{djk}t$ (9.8 or 9.9) respectively. This completes the computation of the concentration expectation value for solute inserted at $\boldsymbol{x}_0 = 0$, $t_0 = 0$. The calculation of the concentration variance can be carried put along the lines of §6 with the aid of the probability density function of displacements of two particles. We have shown, however, that for a solute body whose initial extent is small compared with l_Y and for a limited, but large, time interval, the concentration variance can be related to X_{jk} by (6.8). This equation is valid for X_{jk}^c as well, and we shall limit §§10 and 11 to illustrating the effect of conditioning upon X_{jk}.

10. Illustration of results for conductivity conditioning

We wish to illustrate the general approach by computing effectively the conditional covariance X^c_{jk}. Towards this goal we adopt the exponential covariance C_Y (4.1) and the associated first-order unconditional covariance $C_{Y\phi}$ and variogram (4.2, 4.3).

For the sake of simplicity we shall examine the influence of conductivity conditioning at an isolated point $x_1(x_1, y_1)$. In the case of conductivity conditioning solely, $\mu_k = A = 0$ in (8.4) and only the first M equations have to be maintained. It is seen that for $M = 1$ we get

$$\lambda_1(x) = \frac{C_Y(x, x_1)}{\sigma_Y^2} = c_Y(x, x_1), \tag{10.1}$$

whereas from (8.8) we have

$$\lambda_1'(x) = \frac{C_{\phi Y}(x, x_1)}{\sigma_Y^2} = c_{\phi Y}(x, x_1). \tag{10.2}$$

Since c_Y (4.1) and $c_{Y\phi}$ (4.2) are given explicitly, so are the coefficients of (10.1) and (10.2). The mean $m^c_Y(x)$ (8.1) and $m^c_\phi(x)$ (8.5) can be written as known functions of x, x_1 and Y_1', and on this basis we can calculate the average displacement of a particle released at $x_0 = 0, t_0 = 0$ by (9.6) or (9.7). We are interested here mainly in evaluating the displacement covariances, which are based on the conditional covariances (8.2), (8.5) and (8.9):

$$\left.\begin{aligned} C^c_Y(x, x') &= \sigma_Y^2[c_Y(x, x') - c_Y(x, x_1)\, c_Y(x', x_1)], \\ C^c_{Y\phi}(x, x') &= \sigma_Y^2[c_{Y\phi}(x, x') - c_Y(x, x_1)\, c_{\phi Y}(x', x_1)], \\ \Gamma^c_\phi(x, x') &= \sigma_Y^2[\gamma_\phi(x, x') + c_{\phi Y}(x, x_1)\, c_{\phi Y}(x', x_1)]. \end{aligned}\right\} \tag{10.3}$$

Substitution of (10.3) into the velocity covariances (9.3, 9.4) and subsequent integration in (9.9) with $x = t'$, $y = 0$, $x' = t''$, $y' = 0$ yields the displacement covariances $X^c_{jk}(t)$, which could be calculated in a closed analytical form for the selected C_Y (4.1).

To grasp the effect of conductivity conditioning, we have represented in figure 4 $X_{11}(t)$ (4.5), as well as $X^c_{11}(t)$ (9.9) for conditioning at three different points on the x-axis, i.e. on the line that leads to the largest impact upon X^c_{11}. The selected coordinates of these points were $y_1 = 0$ and $x_1 = 0, 5, 10$. Furthermore, on the same figure the cumulative effect of the three points is also represented by neglecting the interaction between them.

It is seen that conditioning of conductivity at an isolated point has a modest effect, and even the reduction of X_{11} due to an array, at a spacing equal to five times the conductivity integral scale, is no more than 50 %. Since the concentration coefficient of variation for a small solute body (6.9) depends on X^1_{11}, the corresponding reduction due to conditioning is even smaller. It is therefore seen that conductivity conditioning can be used effectively as a mean to reduce the concentration uncertainty, but the measurements have to be carried out on a grid more dense than that of figure 4 in order to achieve significant effects. The asymptotic effect of conditioning at an isolated point is constant and the covariance reduction is of the order of 3.5 (figure 4 for $t \to \infty$). Thus, if we neglect the interaction between points, the distance between the measurement points in the array has to be roughly 1.5 conductivity integral scales in order to reduce the covariance to zero. This is of course not exactly true as the effectiveness of conditioning decreases because of the interaction between close measurement points, but it is fair to presume that significant reduction of X_{11} will

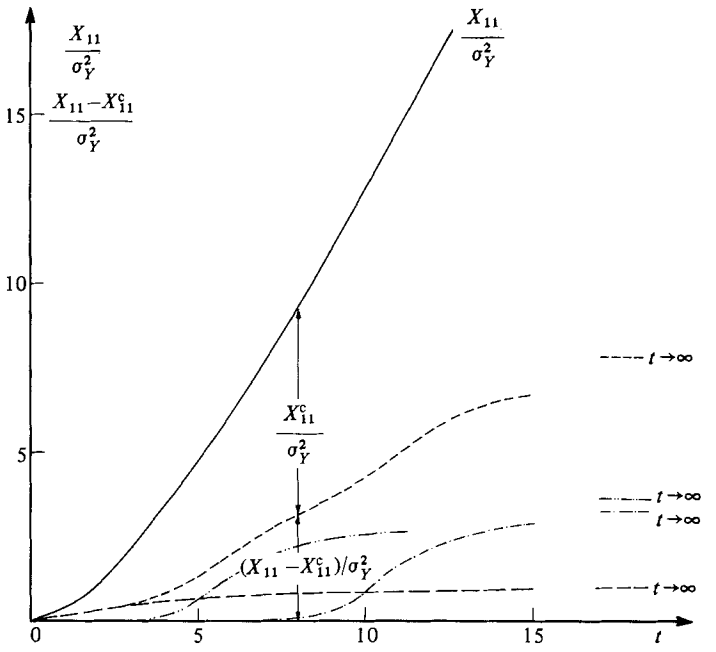

FIGURE 4. The unconditional X_{11} and conditional $X_{11}-X_{11}^c$ displacement longitudinal covariances for two-dimensional flow. Conditioning by conductivity at a point of coordinate $\boldsymbol{x}_1(x_1, y_1)$. ——, (4.5); — — —, (9.9) for $x_1 = 0, y_1 = 0$; – · –, (9.9) for $x_1 = 5, y_1 = 0$; – · · –, (9.9) for $x_1 = 10, y_1 = 0$; – – – –, cumulative effect for the previous three.

occur only if the distance is smaller than $2I_Y$. A complete computation can be carried out along the lines of §8, the only additional complication being the need to invert the matrix $C_Y(\boldsymbol{x}_j, \boldsymbol{x}_k)$.

Conditioning at points on the x-axis has not effect upon the lateral covariance X_{22}. We have considered instead conditioning at two points at same $x_1 = x_2$, and $y_1 = -y_2$. The maximum reduction is achieved for $y_1 = 2$, and we have represented in figure 5 $X_{22}(t)$ (4.6), as well as $X_{22}^c(t)$ (9.9), for $x_1 = 5$ and $y_1 = -y_2 = 2$, this time the interaction between the two points being taken into account. It is seen that the effect upon covariance reduction is quite small. Introducing two more points at same $x_1 = 5$ and $y_3 = -y_4 = 1$ improves the picture, but still the reduction is both localized and modest. Again, a grid with distances between pairs of measurement points smaller than two conductivity scales in the x-direction is needed in order to achieve a considerable reduction of the lateral covariance and subsequently of the concentration variance.

Summarizing this section, it is seen that transmissivity conditioning has two main effects. First, the concentration expectation value is still Gaussian and satisfies the convection–dispersion equation, but the average convective velocity is no more constant and equal to unity. For a single particle the centroid of the mean concentration distribution will move in the space along a sinuous path, given by (9.6, 9.7), which is influenced by the location of conductivity measurement points, as well as by its actual values. Secondly, the concentration coefficient of variation is diminished by conditioning. The extreme conceivable case is the one in which the measurement points are so dense that the transport becomes deterministic and uncertainty disappears. It is one of the major features of conditional probability that a smooth transition is achieved from this extreme case to the one of unconditional

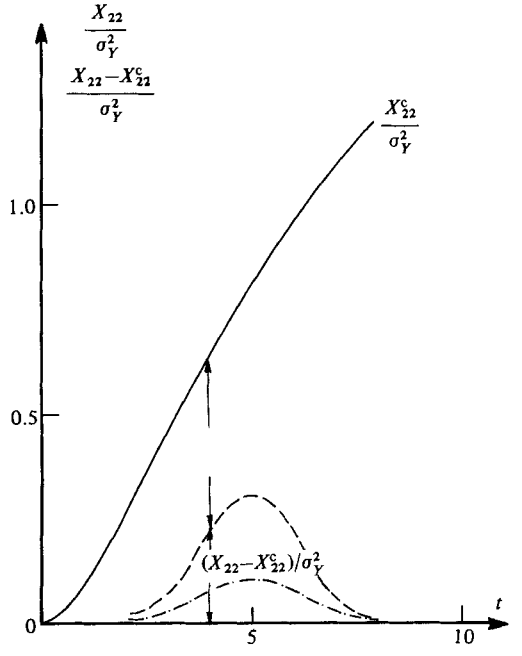

FIGURE 5. The unconditional X_{22} and conditional $X_{22}-X_{22}^c$ displacement lateral covariances for two-dimensional flow. Conditioning by conductivity at two points of coordinates $x_1 = x_2$, $y_1 = -y_2$. ——, (4.6); –·–·–, (9.9) for $x_1 = 5$, $y_1 = 2$; – – –, (9.9) and conditioning at four points $x_1 = x_2 = x_3 = x_4 = 5$, $y_1 = -y_2 = 2$, $y_3 = -y_4 = 1$.

transport. The examples of figures 4 and 5 give an indication of the covariance reduction in a few cases. The methodology applied here, however, permits one to investigate in a systematic manner the worth of measurements on grids of various densities in reducing uncertainty. The simple examples given here indicate that distances smaller than, say, two transmissivity integral scales are needed in order to reduce uncertainty significantly. These conclusions are valid for the time interval in which dispersion by local effect has a limited effect, and this time may be quite large.

The case of transport of an initially finite body or for a continuous plume is more complex and in general requires solution by numerical quadratures.

11. The influence of head conditioning upon the concentration field

Our last topic is the investigation of the effect of measurement of the head ϕ at a few points, the simplest case being that of two points, since it can be shown that head conditioning at an isolated point has no influence upon transport. The computations are quite similar to those of §10, and we shall address directly the question of reduction of the two-dimensional covariances X_{11} and X_{22}. Under the same assumptions as in §9, we start now with (8.4) and (8.8) in which $\lambda_j = \lambda_j' = 0$ and only the last $N-M$ equations are maintained with $M = 0$, $N = 2$.

The first case to consider is of two points lying on the x-axis, i.e. on the mean trajectory. To simplify matters further and to assess the greatest impact of conditioning, we assume that the two points are close, i.e. at a distance that is small compared with the conductivity integral scale. This can be called a head doublet and it provides the magnitude of the longitudinal head gradient (the points should not

be too close to avoid large measurement errors). Taking the limit $x_1 - x_2 \to 0$ and after a few manipulations we obtain

$$\lim_{x_1-x_2\to 0} r_\phi(x_1-x_2,0) = \tfrac{3}{16}(x_1-x_2)^2, \tag{11.1}$$

$$X_{11}^c(t) = X_{11}(t) - \tfrac{8}{3}\sigma_Y^2\left[c_{Y\phi}(x_1-t,0) - c_{Y\phi}(x_1,0) + \frac{\partial\gamma_\phi(x_1-t,0)}{\partial x_1} + \frac{\partial\gamma_\phi(x_1,0)}{\partial x_1}\right]^2. \tag{11.2}$$

For the exponential correlation (4.1) the two functions $C_{Y\phi}$ and γ_ϕ are given by (4.2) and (4.3) respectively, and X_{11}^c (11.2) can be calculated explicitly. This has been done for $x_1 = 5$ and $x_1 = 10$, and the results are represented in figure 6, together with the covariance reduction caused by a conductivity measurement point at the same locations. Inspection of figure 6 reveals that the reduction of the longitudinal covariance by a head doublet is much smaller than that of a conductivity measurement and is localized.

In a similar manner we have evaluated the effect upon the lateral covariance of two conditioning points at $x_1 = 5$ and $y_1 = -y_2$ to obtain

$$X_{22}^c(t) = X_{22}(t) - \frac{\sigma_Y^2}{2\gamma_\phi(x_1-x_2)}\left[\frac{\partial\gamma_\phi(x_2-t,y_2)}{\partial y_2} - \frac{\partial\gamma_\phi(x_1-t,y_1)}{\partial y_1} - \frac{\partial\gamma_\phi(x_2,y_2)}{\partial y_2} + \frac{\partial\gamma_\phi(x_1,y_1)}{\partial y_1}\right]^2. \tag{11.3}$$

The covariance reduction is represented in figure 7 for $y_1 = 2$ and $y_1 = 0.5$ respectively. On the same figure the effect of transmissivity conditioning at $x_1 = 5$, $y_1 = -y_2 = 2$ has also been depicted. This time the two types of measurements have comparable magnitudes.

Summarizing this section, it is seen that the impact of head measurements upon the displacement covariances, and henceforth upon concentration variance, is less than that of conductivity conditioning. Again, a systematic study can be carried out by comparing the effects of grids of measurement points of various densities, for transmissivity and heads separately or for a combination of both.

12. Summary of Part 2 and conclusions

In the second part of the study the measured values of the conductivity and head are taken into account directly and the statistical moments of the velocity and concentration fields are computed with the aid of the conditional probability distribution functions of the conductivity and head. Again, this is an option which exists in the case of fixed random structures and which distinguishes it from other cases in which the velocity field is time-fluctuating. The conditional probability allows for a continuous transition between two extreme cases. In the first one, when measurements are available on a dense grid of points at distance much smaller than l_Y, the ensemble average of the velocity varies in an intricate manner throughout the space, whereas the variance tends to zero, so that the field is practically deterministic and uncertainty disappears. At the other extreme we have the unconditional p.d.f. for which the average velocity is constant, but the variances and higher moments may be quite large. These concepts, which are quite common in geostatistics, have been illustrated separately for conductivity and head conditioning. It has been shown that conductivity measurements may reduce considerably the

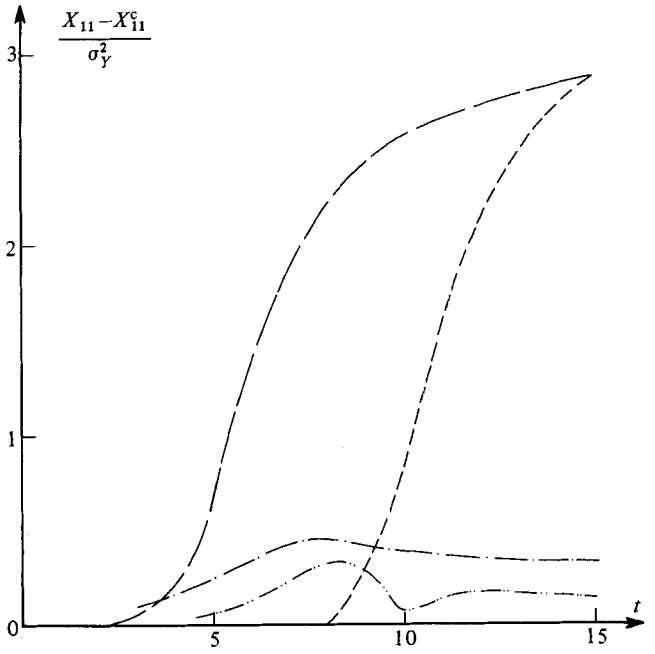

FIGURE 6. Comparison between longitudinal covariance reduction $X_{11}-X_{11}^c$ by conductivity conditioning at one point and by a head-doublet conditioning. ——, (9.9), conductivity at $x_1 = 5$, $y_1 = 0$; – – – – (10.6), conductivity at $x_1 = 10$, $y_1 = 0$; –·–·–, (11.2), head doublet at $x_1 = 5$, $y_1 = 0$; –··–··– (11.2), head doublet at $x_1 = 10$, $y_1 = 0$.

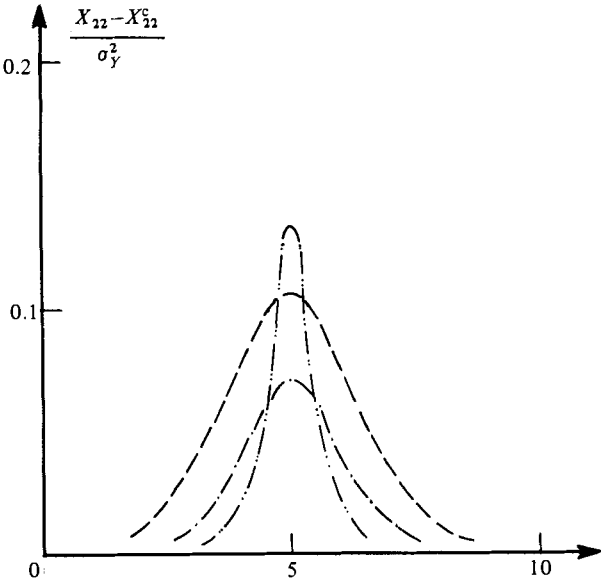

FIGURE 7. Comparison between lateral covariance reduction $X_{22}-X_{22}^c$ by conductivity conditioning and head conditioning at two points. ———, (9.9), conductivity at $x_1 = x_2 = 5, y_1 = -y_2 = 2$; –·–·–, (11.3), head at $x_1 = x_2 = 5$, $y_1 = -y_2 = 2$; –··–··–, (11.3) head at $x_1 = x_2 = 5$, $y_1 = -y_2 = 0.5$.

uncertainty in the prediction of concentration, if measurement points belong to an array with distance between them smaller than, say, two conductivity integral scales. The head conditioning has been shown to have less impact upon concentration variance.

It is suggested that a similar methodology can be employed for other problems of transport by random fluid motions in which the correlation scale of the velocity field is much larger than that of the solute body.

I am indebted to G. K. Batchelor for his helpful comments.

REFERENCES

BERAN, M. J. 1968 *Statistical Continuum Theories*. Interscience.

BUYEVICH, YU. A., LEONOV, A. J. & SAFRAI, V. M. 1969 Variations in filtration velocity due to random large-scale fluctuations of porosity. *J. Fluid Mech.* **37**, 371–381.

CLIFTON, P. M. & NEUMAN, S. P. 1982 Effects of kriging and inverse modeling on conditional simulation of the Avra Valley aquifer in Southern Arizona. *Water Resources Res.* **18**, 1215–1237.

DAGAN, G. 1982*a* Stochastic modeling of groundwater flow by unconditional and conditional probabilities, 1. Conditional simulation and the direct problem. *Water Resources Res.* **18**, 813–833.

DAGAN, G. 1982*b* Stochastic modeling of groundwater flow by unconditional and conditional probabilities, 2. The solute transport. *Water Resources Res.* **18**, 835–848.

DELHOMME, J. P. 1979 Spatial variability and uncertainty in groundwater flow parameters: a geostatistical approach. *Water Resources Res.* **15**, 269–280.

DEVARY, J. L. & DOCTOR, P. G. 1982 Pore velocity uncertainties estimation. *Water Resources Res.* **18**, 1157–1164.

FREEZE, R. A. 1975 A stochastic-conceptual analysis of one-dimensional groundwater flow in nonuniform homogeneous media. *Water Resources Res.* **11**, 725–741.

FRIED, J. J. & COMBARNOUS, M. A. 1971 Dispersion in porous media. *Adv. Hydrosci.* **7**, 169–282.

GELHAR, L. J. & AXNESS, C. L. 1983 Three-dimensional stochastic analysis of macrodispersion in aquifers. *Water Resources Res.* **19**, 161–180.

GELHAR, L. W., GUTJAHR, A. L. & NAFF, R. L. 1979 Stochastic analysis of macrodispersion in a stratified aquifer. *Water Resources Res.* **15**, 1387–1397.

JOURNEL, A. G. & HUIJBREGTS, C. J. 1978 *Mining Geostatistics*. Academic Press.

LALLEMAND-BARRÉS, P. & PEAUDECERF, P. 1978 Recherche des relations entre la valeur de la dispersivité macroscopique d'un milieu aquifère, ses autres caracteristiques et les conditions de mesure. Etude bibliographique. *Bull. BRGM., section* III no. 4, 277–284.

MATHÈRON, G. & DE MARSILY, G. 1980 Is transport in porous media always diffusive? A counterexample. *Water Resources Res.* **16**, 901–917.

MOOD, A. M. F. & GRAYBILL, F. A. 1963 *Introduction to the Theory of Statistics*, 2nd edn. McGraw-Hill.

PHYTHIAN, R. 1975 Dispersion by random velocity fields. *J. Fluid Mech.* **67**, 145–153.

SIMMONS, C. S. 1982 A stochastic-convective ensemble method for representing dispersive transport in groundwater. *EPRI Palo-Alto*, Calif., *Tech. Rep.* CS-2558 RP1406-1.

SMITH, L. & SCHWARTZ, F. W. 1980 Mass transport, 1. Stochastic analysis of macro-dispersion. *Water Resources Res.* **16**, 303–313.

SUDICKY, E. A., CHERRY, J. A. & FRIND, E. O. 1980 Hydrologic studies of a sandy aquifer at an abandoned land fill, Part 4. A natural gradient tracer test. *Rep. under Contract* OSU79–00195, *Dept Earth Sci. Univ. Waterloo.*

TAYLOR, G. I. 1921 Diffusion by continuous movements. *Proc. Lond. Math. Soc.* (2) **20**, 196–212.